Applied Environmental Biotechnology

RESERACH ARTICLE

Fe^{2+} and Zn^{2+} Single and Competitive Biosorption from Binary Metal Solution Using Phosphoric Acid-Activated Cashew Nutshell to Minimize Ecotoxicity

Yusufu Luka*, Abdulhalim Musa Abubakar, Abubakar Yusuf Waziri, Aminu Girei Lauwalu

Department of Chemical Engineering, Faculty of Engineering, Modibbo Adama University, Yola, Adamawa State, Nigeria

Abstract

Metal contamination in water bodies is usually present as multiple metals rather than a single metal, and the excess of zinc (Zn) and iron (Fe) in particular affects human health and industrial equipment performance. In order to solve the challenges with metallic oxide adsorbents for removing these metals from water, this study sought to utilize cashew nutshell activated carbon (CNS-AC), activated using phosphoric acid (H_3PO_4), for their individual and simultaneous/competitive sorption. Two cases involving a bimetallic solution of initial concentration (C_o) between 5 and 200 mg/L and the one dosed with 4–40 g/L of CNS-AC adsorbent were analyzed at Zn:Fe ratios of 1:1.3, 1.7:1, and 1:2.6. The variations were tested against the removal efficiency (RE) and adsorption capacities (q_e) of Zn, Fe, or Zn-Fe mono- or competitive sorption, as H_3PO_4 activation promotes higher pore development and surface area. Fourier transform infrared (FTIR), scanning electron microscopy (SEM), and atomic absorption spectrophotometry were conducted pre- and/or post-sorption by CNS-AC to determine the functional groups, morphology, and ion concentrations. Findings show that a 603.36 cm^{-1} peak implied an adsorbent-metal interaction by FTIR and a smooth texture microstructure by SEM. For all ratios, the lower the C_o, the higher the RE for single and co-sorption, and the lower the q_e for mono-sorption of ions. On the other hand, the optimal doses of 40 g/L corresponds to a maximum RE of approximately 28.97% across all Zn-Fe ratios for individual and multiple ion removal. Considering the doses, the 1.7:1 ratio is the most effective in terms of RE and q_e, while 1:1.3 ratio effectively removes Zn+Fe under changing C_o. The findings generally depict a moderate adsorption process with room for further improvement. Because the presence of Zn and Fe in water that is generally suitable for drinking, industrial use, and equipment safety, it must be < 1 and < 0.05 mg/L, respectively. Compared to hydrochloric and nitric acids, H_3PO_4 is less corrosive and environmentally safer, as it produces fewer toxic fumes.

Keywords: Cashew nutshell, Iron sorption, Zinc sorption, Competitive adsorption, Phosphoric acid

***Corresponding author:**
Yusufu Luka
(sufuluka@mau.edu.ng)

Citation: Luka, Y., Abubakar, A. M., Waziri, A. Y., & Lauwalu, A. G. Fe^{2+} and Zn^{2+} Single and Competitive Biosorption from Binary Metal Solution Using Phosphoric Acid-Activated Cashew Nutshell to Minimize Ecotoxicity. *Applied Environmental Biotechnology*. http://doi.org/10.26789/AEB.2026.01.003

Received: July 15, 2026

Revised: September 21, 2026

Accepted: October 30, 2026

Published online: November 16, 2026

Copyright: © 2026 Author(s). This is an Open-Access article distributed under the terms of the Creative Commons Attribution License, permitting distribution, and reproduction in any medium, provided the original work is properly cited.

Publisher's Note: AccScience Publishing remains neutral with regard to jurisdictional claims in published maps and institutional affiliations.

1. Introduction

Oxides of aluminum (Al), manganese (Mn), and iron (Fe) (Fungaro & Graciano, 2007; Kalbasi *et al*., 1978; Krok *et al*., 2022; Trivedi & Axe, 2001), as well as iron(III) oxyhydroxide (FeO(OH)), also known as ferric oxyhydroxide (Benjamin & Leckie, 1981a, 1981b; Madrid *et al*., 1991; Millward & Moore, 1982; Tessier *et al*., 1985), and hydrous ferric oxides (HFO) (Kinniburgh & Jackson, 1982; Musić & Ristic, 1992; Shuman, 1977), are good adsorbents for zinc (Zn). Ponthieu *et al*. (2006) listed the metal ions that can be adsorbed by iron oxides (such as hematite, magnetite, goethite, and ferrihydrite), but excluded Fe. Arsenic removal from water has also been successfully carried out using an Fe- and Al-based adsorbent, as reviewed by Giles *et al*. (2011). Ferrihydrite is a poorly crystalline iron(III) oxyhydroxide characterized by a high specific surface area and considerable adsorption capacity for Fe ions (Fe^{2+} & Fe^{3+}), if the surface is not already saturated with Fe. Potential limitations of using iron oxides, FeO(OH), and HFO for Zn and Fe removal from aqueous solutions include rapid saturation of adsorption sites; the formation of additional iron oxides through Fe^{2+} oxidation, which block active sites; transformation of HFO into more stable stable mineral phases, such asgoethite and hematite; preferential adsorption of Fe^{3+} over Zn^{2+}; and difficulties associated with desorbing retained metals. Studies have shown that their adsorption efficiency is highly pH-sensitive, as low pH reduces adsorption by causing the dissolution of iron oxides, while high pH leads to the precipitation of $Zn(OH)^2$ or $Fe(OH)_3$ instead of adsorption (Srivastava *et al*., 2005). The foregone challenges cancel out the candidacy of the foregone adsorbents for ridding water of Zn and Fe efficiently. A careful assessment show that activated cashew nutshell (CNS) adsorbent is a superior alternative to iron-based adsorbents due to higher efficiency, cost-effectiveness, renewability, and stability in diverse water treatment applications, in an exact opposite of the weaknesses listed.

Table 1 shows that many adsorbents categorized into natural materials, synthetic composites, agricultural byproducts, and industrial residues are capable of simultaneously adsorbing multiple metal ions, starting from their presence in binary, ternary, and multicomponent mixtures involving either Zn or Fe or both. Literature evidence in Table 1 shows that natural adsorbents dominate research interest compared to engineered ones (modified materials, nanomaterials, and functionalized composites), simply due to their abundance, cost-effectiveness, and eco-friendliness. An obvious research gap is the non-use of CNS, which boosts the mentioned merits for the competitive adsorption of Zn and Fe in binary mixtures. Competitive adsorption studies on Fe are less relevant and scantily reported (see Table 1), as Fe removal is often governed by precipitation rather than adsorption. It will be difficult to differentiate between adsorbed Fe and background Fe if the adsorbent used contains Fe. CNS contain Zn and Fe in trace amounts and can be leached out via acid/base treatments during activation or carbonization/pyrolysis. Kouakou *et al*. (2013) reported the use of commercial activated carbon (AC) in a manner similar to the study herein to remove Zn and Fe individually, without considering their simultaneous sorption.

Zn and Fe can interact during intestinal absorption, with competition occurring at the intestinal mucus layer, as investigated by Einhorn *et al*. (2024). High levels of Zn can lead to stomach cramps, nausea, vomiting, and long-term immune system suppression. Its toxicity affects aquatic organisms, causing growth defects, reproductive issues, and mortality in fish and plants. Elevated Zn concentrations may impart a metallic taste to drinking water and adversely affect its aesthetic quality. On the other hand, Fe-rich water can promote bacterial growth (especially iron bacteria) and eutrophication, and its excessive intake could trigger liver damage, diabetes, and hemochromatosis (iron overload disease). Additionally, Fe causes a reddish-brown stain in plumbing fixtures, sinks, and clothes. In boilers and cooling towers, Fe and Zn form deposits that reduce heat transfer efficiency and increase energy consumption, in addition to their potential for pipe scaling and clogging. Both make water aesthetically unappealing if present in high amounts by causing turbidity and discoloration. Drinking-water quality guidance and regulations issued by organizations and authorities, including the World Health Organization, the United States Environmental Protection Agency, and the European Union Drinking Water Directive, address metal concentrations and other water-quality parameters, and their exceedance will require adsorption, precipitation, or membrane filtration treatment methods. Preferably, channeling the recovered metals from water to other uses is advisable, as the individual (except Zn) and bi-metal systems of Zn and Fe are capable of adsorbing diverse contaminants. For instance, a Zn-Fe system (i.e., Zn-Fe/Al_2O_3) could serve as a good adsorbent for hydrogen sulphide (H_2S) in biogas, according to Yan *et al*. (2024); enrofloxacin can be eliminated from water using functionalized biochar of Fe-Zn bimetallic oxide (Hong *et al*., 2024) and; the removal of organic pollutant using magnetic carbon nanorods derived from Zn/Fe mixed-metal MOF-74 (Del Rio *et al*., 2022). Pollutants can be adsorptively removed by Fe-based materials (Islam *et al*., 2024), which may be in form of zero-valent iron (Fe^0) for the removal of As (Bang *et al*., 2005; Chai *et al*., 2022; Edward *et al*., 2023; Kanel *et al*., 2005; Pepler, 2009; Rahmani *et al*.,

Table 1. Previous Use of Adsorbents for Competitive Adsorption of Bi- & Multi-Metals Solution Involving Zn or Fe

Multi-metals system	Adsorbent	Source
Zn & Mn	Alginate-iron oxide-combusted coal gangue composite	(Mohammadi *et al.*, 2021)
Zn & Mn	Iron oxide-combusted coal gangue composite	(Mohammadi *et al.*, 2020)
Zn & Mn	Alginate-combusted coal gangue composite	(Mohammadi *et al.*, 2019)
Zn & Cd	Nano-iron and titanium oxides	(Sepehr *et al.*, 2022)
Zn & Cd	Granular activated carbon	(Gabaldón *et al.*, 1996)
Zn & Cd	Acid and alkaline soils	(Ming *et al.*, 2016)
Zn & Cd	Cork stopper particles	(Ebrahime & Alsaade, 2019)
Zn & Cd	Soil	(Niu *et al.*, 2018)
Zn & Cd	V, Ti-bearing magnetite-humic acid	(M. Lu *et al.*, 2021)
Zn & Cd	Biochar, loess, and biochar–loess mixture	(Y. W. Li *et al.*, 2024)
Zn & Cd	Aluminum oxide nanoparticles	(Stietiya & Wang, 2014)
Zn & Cd	Soil series	(Azura *et al.*, 2012)
Zn & Cd	Palm kernel shell activated carbon	(Muhammad *et al.*, 2011)
Zn, Cu & Cd	Granular Fe-Mn binary oxide	(Du *et al.*, 2021)
Zn, Cu & Cd	Water purification plant sludge granules	(Du *et al.*, 2020)
Zn, Cu & Cd	Ferronickel slag	(Seo *et al.*, 2016)
Zn, Cd, Cu & Pb	Highly-weathered Brazilian soils	(Fontes *et al.*, 2000)
Zn, Cd, Cu & Pb	Eastern China soils	(S. G. Lu & Xu, 2009)
Zn, Cd, Cu & Pb	Oxygen furnace slag	(Y. Xue *et al.*, 2009; Y. Xue, *et al.*, 2020)
Zn, Cd, Cu & Pb	2-Line ferrihydrite	(Rout *et al.*, 2012)
Zn, Cd, Cu & Pb	Composted livestock waste	(M. Zhang *et al.*, 2017)
Zn, Cd, Cu & Pb	Kaolinite	(Srivastava *et al.*, 2005)
Zn, Cd, Cu & As	Thermal desorption residue from oil sludge-contaminated soil	(G. Zhang *et al.*, 2022)
Zn, Cd, As & Pb	Mg–Al layered double hydroxide	(Mo *et al.*, 2024)
Zn, Cd, Hg & Pb	Dumbbell- and flower-shaped potato starch phosphate polymer	(Bashir *et al.*, 2020)
Zn, Cd & Pb	L-arginine modified magnetic bioadsorbent (Fe_3O_4-CS-L)	(Guo *et al.*, 2017)
Zn, Cd & Pb	Tunisian smectite	(Eloussaief *et al.*, 2013)
Zn, Cd & Pb	*Eichhornia crassipes*	(Mahamadi & Nharingo, 2010)
Zn, Cd & Pb	Magnetic silica gel	(Guo *et al.*, 2018)
Zn, Cd & Pb	Natural & Fe(III)-modified zeolites	(Mihajlović *et al.*, 2015)
Zn, Cd & Pb	Velvet bean (*Stizolobium Aterrimum*)	(Santos *et al.*, 2014)
Zn, Cd & Pb	Rice husk & wood chip biochar	(Lee & Shin, 2021)
Zn, Cu & Pb	Francisco Beltrão soil (dystrophic Red Latosol or Oxisol) & São Pedro do Paraná (Red-Yellow Argisol Abruptic eutrophic) in Brazil	(Kummer *et al.*, 2018)
Zn, Cu & Pb	Luvisol profile	(Sipos, 2009)
Zn, Cu & Pb	Hydroxyapatite-biochar nanocomposite	(Y.-Y. Wang *et al.*, 2018)
Zn, Cu & Pb	Polymeric Al/Fe modified clinoptilolite	(H. Y. Wang & Huang, 2010)

(*Cont'd...*)

Table 1. (*Continued*)

Multi-metals system	Adsorbent	Source
Zn, Cu & Pb	Spent mushroom compost biochar	(Abdallah *et al*., 2019)
Zn, Cu & Pb	Amidoxime-functionalized polypropylene fiber	(Zhao *et al*., 2020)
Zn, Cu & Pb	Residual soil-derived zeolite	(Z. Wang *et al*., 2023)
Zn, Cu & Pb	δMnO_2	(Catts & Langmuir, 1986)
Zn, Cu & Pb	Goethite	(Perelomov *et al*., 2011)
Zn, Cu & Pb	Sugarcane cellulose	(F. Wang *et al*., 2017)
Zn, Cu, Pb & Ni	Chilean soils (Diguillin & Ralun)	(Cazanga *et al*., 2008)
Zn, Cu & Hg	Banana peels calcined magnetic biochar	(Oladipo *et al*., 2019)
Zn, Cu & Mn	Calcareous soils	(Al-Hamandi *et al*., 2024)
Zn, Pb & Mn	Nano-Fe_2O_3 particles	(Youssef *et al*., 2017)
Zn, Cu & Ni	Dissolved organic matter	(Refaey *et al*., 2017)
Zn, Cu & Ni	Cork powder	(Chubar *et al*., 2003)
Zn & Ni	Iron oxide- and manganese oxide-coated sand	(Choi *et al*., 2020)
Zn, Cd & Ni	Tourmaline	(H. Liu *et al*., 2013)
Zn, Cd & Ni	Commercial carbons modified with eggshell wastes	(Guijarro-Aldaco *et al*., 2011)
Zn, Cd, Cu & Ni	Brazilian humid-tropical region soils	(Moreira & Alleoni, 2010)
Zn, Cd, Cu & Ni	Iron oxide nanoparticles	(Ebrahim *et al*., 2016)
Zn, Cd, Cu & Ni	Mine soil amended with mussel shell	(Garrido-Rodriguez *et al*., 2014)
Zn, Cd, Cu & Ni	Nanoparticle-treated vineyard soils	(Beygi *et al*., 2023)
Zn, Cd, Cu & Ni	Multi-carboxyl-functionalized silica gel	(M. Li *et al*., 2014)
Zn, Cd, Cu & Ni	Palygorskite and sepiolite silicate clay minerals	(Sheikhhosseini *et al*., 2013)
Zn, Cd, Cu, Ni & Pb	Kaolinite	(Gu & Evans, 2008)
Zn, Cd, Cu, Ni & Pb	Fithian illite	(Gu & Evans, 2007)
Zn, Cd, Cu, Ni & Pb	Alkali-modified biochar	(Ding *et al*., 2016)
Zn, Cd, Cu, Ni & Pb	Peanut shell biochar	(Shan *et al*., 2020)
Zn, Cd, Cu, Pb & Co	FAU-type zeolites	(Joseph *et al*., 2020)
Zn, Cd, Cu & Co	Agricultural and greenhouse soils	(Jalali *et al*., 2024)
Zn & Co	Brown coal fly ash-derived zeolitic material	(Pipíška *et al*., 2019)
Zn, Co, Cu & Ni	Hydrous manganese dioxide	(Kanungo *et al*., 2004)
Zn, Co, Mn & Ni	Hydrous oxides of iron (βFeOOH)	(Kanungo, 1994)
Zn, Cd & Cr	Orange waste	(Pérez-Marín *et al*., 2024)
Zn, Cd, Cu, Cr, Pb & Ni	Humic Umbrisols	(Covelo *et al*., 2004)
Zn, Cd, Cu, Cr, Pb & Ni	Coconut coir fiber, blast furnace slag, waste tire crumb rubber, biochar & iron-coated biochar	(Esfandiar *et al*., 2022)
Zn, Cd, Cu, Cr, Pb & Ni	Clay-bearing mining wastes	(Helios-Rybicka & Wójcik, 2012)
Zn, Cd, Cu, Cr & Pb	Iron-coated Australian zeolite	(Nguyen *et al*., 2015)
Zn, Cd, Cu, Mn, Pb & Ni	Calcareous soils	(Jalali & Moradi, 2013)
Zn & Cu	Acid soils	(Pérez-Novo *et al*., 2008)
Zn & Cu	Sandy soil	(Mesquita *et al*., 2002)
Zn & Cu	Calcareous soils	(Mesquita *et al*., 2000)

(*Cont'd...*)

Table 1. (***Continued***)

Multi-metals system	Adsorbent	Source
Zn & Cu	Bt horizon of a Savanna Alfisol	(Agbenin & Olojo, 2004)
Zn & Cu	Algerian bentonite	(Bouazza *et al*., 2018)
Zn & Cu	Coffee waste	(Agwaramgbo *et al*., 2017)
Zn & Cu	*Tetradesmus obliquus*	(Wei *et al*., 2024)
Zn & Cu	Soil samples (Dystryc Fluvisols, Gleyic Podzol & Haplic Luvisol)	(Mesquita & e Silva, 2002)
Zn & Cu	Sandy soil	(Mesquita & Carranca, 2005)
Zn & Cu	Carbonized food waste	(Han *et al*., 2012)
Zn & Cu	Natural clay	(Sdiri *et al*., 2014)
Zn & Cu	Acid soils	(Fernández-Calviño *et al*., 2010)
Zn & Cr	Steel slag	(Chen *et al*., 2019)
Zn, Cu & Cr	Corn-cob ash	(Ugwu & Agunwamba, 2022)
Zn, Cu & Cr	Wine-processing waste sludge	(C.-C. Liu *et al*., 2009)
Zn & Pb	Animal-derived biochar	(C. Xue *et al*., 2020)
Zn & Pb	Termite mound	(Abdus-Salam & Bello, 2015)
Zn & Pb	Van apple pulp activated carbon	(Depci *et al*., 2012)
Zn & Pb	Humus-like substances modified montmorillonite	(Jiang *et al*., 2021)
Fe, Cu & Ni	Soil-based media	(Bode, 2023)
Fe & Mn	Lignite	(Mohan & Chander, 2006)
Fe & Mn	Green tomato husk	(García-Mendieta *et al*., 2012)
Fe & Cr	*Chlorella vulgaris* and *Rhizopus arrhizus*	(Sağ *et al*., 1998)
Fe & Cr	*Rhizopus arrhizus*	(Sağ & Kutsal, 1996)
Fe, Zn & Cu	Steel slag	(Yang *et al*., 2024)
Fe, Zn & Pb	Polyvinyl alcohol grafted chitosan variant resins	(Patel *et al*., 2023)
Fe, Zn, Pb & Cu	Oil palm fibers biochar	(Ighalo *et al*., 2020)
Fe, Zn, Pb & Cd	Nanostructured ash cedar	(Hafshejani *et al*., 2015)

2011; Wu *et al*., 2021; Zhu *et al*., 2020), Cr^{6+} (Choudhury *et al*., 2024), Cd (Z. Wang *et al*., 2020), Pb (Sepehri *et al*., 2023), Cu (Tarekegn *et al*., 2021), and nitrates (Gibert *et al*., 2022; Lv *et al*., 2022). All these contribute to ecotoxicity control.

This study strives to harness CNS for adsorptive single- and competitive removal of Zn and Fe from water. Previously, it has been used to attenuate Pb (Kumar, Ramalingam, Abhinaya, *et al*., 2011), Cu (SenthilKumar *et al*., 2011), Ni (Kumar, Ramalingam, Kirupha, *et al*., 2011), Cr (De Oliveira *et al*., 2021), and Zn (Kumar *et al*., 2012) from water, after treating with sodium hydroxide (NaOH) (De Oliveira *et al*., 2021), sulfuric acid (H_2SO_4) (Kumar, Ramalingam, Abhinaya, *et al*., 2011), and phosphoric acid (H_3PO_4). The use of H_3PO_4 for sorbent activation was similarly carried out for the mono-sorption of Zn using CNS-AC by Luka *et al*. (2024). The present selection of H_3PO_4 for activating the CNS adsorbent in this study is favored by the fact that pore blockage caused by excessive carbonization with the use of H_2SO_4 is avoided. Non-optimal adsorption due to the creation of fewer micropores and more mesopores associated with NaOH activation is not a concern. Basically, H_3PO_4 introduces phosphate functional groups ($-PO_4^{3-}$) that enhance chelation and ion exchange for Zn^{2+} and Fe^{2+} removal compared to $-SO_4^{2-}$ and -OH groups. Due to moderate-temperature support by H_3PO_4 activation, it preserves the CNS structure and minimizes excessive decomposition, as against H_2SO_4, which is highly corrosive and aggressive or NaOH that

causes adsorbent lifespan reduction through swelling and structural weakening. In line with environmental friendliness, H_3PO_4 is less corrosive and generates fewer toxic byproducts (Table 2) and do not cause alkaline wastewater observable in the use of NaOH.

Shan *et al.* (2020) experimented with the competitive adsorption of Zn and other metal ions at varying initial concentrations of metals (C_o) and adsorbent dose. Herein, the empirical study is divided into two cases. Case 1 involved the analysis of the removal efficiency (RE) and adsorption capacity (q_e) of single and co-sorption of Zn and Fe in a solution containing the metals at ratios of 1:1.3, 1.7:1, and 1:2.6 and concentrations between 5 and 200 mg/L. Case 2 adopted the same Zn:Fe ratios but varied the CNS-AC dosage from 4 to 40 g/L. F. Wang *et al.* (2017) previously employed a ratio of 1:1. As carried out in most studies, Fourier transform infrared (FTIR) spectroscopy, scanning electron microscopy (SEM), energy-dispersive X-ray (EDX), and atomic absorption spectrophotometry (AAS) characterization approaches were used to characterize the adsorbent and evaluate the adsorption process. The gap addressed by the current study is the competitive sorption of Zn+Fe from solution. The novelty lies in varying the concentration of the binary solution at different ratios and the use of CNS-AC as an adsorbent.

2. Materials and Methods

2.1. Reagents, Materials, and Equipment

Reagents used in this study include distilled water, deionized water, H_3PO_4, zinc chloride ($ZnCl_2$), NaOH, H_2SO_4, and iron(II) sulfate ($FeSO_4$). CNS was the only organic waste material employed in this work. Using important equipment and apparatus such as an oven, mortar and pestle, orbital shaker, atomic absorption spectrophotometer, plastic bottles, pH meter, turbidity meter, and conductivity meter, Zn and Fe ions were removed from water.

2.2. CNS Preparation and Activation

Cashew nuts were purchased from a local market in Yola, Adamawa State, Nigeria; their shells were collected for adsorbent preparation. Briefly, the shells were thoroughly washed with distilled water to eliminate impurities before drying in the open air for seven days. The washed and dried CNS was allowed to undergo coarse crushing in order to obtain a reduced size. After sieving through standard steel sieves, only fractions with diameters ranging from 0.5 to 1.25 mm were retained and used for the analysis. Next, 10 wt.% H_3PO_4 was used for chemical activation by mixing with the ground CNS before its carbonization. Approximately 30 g of dried CNS was impregnated with 10 wt% H_3PO_4 solution at a precursor-to-solution ratio of 1:1 and left for 30 min at room temperature. The impregnated sample was then placed in an oven at 110 °C for 24 h. Pyrolysis of the impregnated sample was carried out for 1 h in a carbolite furnace in the absence of air (oxygen) by preheating to an initial room temperature of 27 °C and then to a final temperature of 600 °C, at a heating rate of 10 °C min^{-1}. It was then allowed to cool down to ambient temperature, after which a dry residue was obtained. A total elimination of phosphate ions (PO_4^{3-}) from the H_3PO_4-activated CNS sample was achieved through abundant washing with distilled water until a neutral pH was observed, as reported in Srivastava *et al.* (2005). The resultant AC of the CNS sample was then oven-dried at 110 °C for a period of 24 h. The final CNS-AC material sample was further ground and then sieved to obtain particles with diameters < 71 µm, which were later used as the metal ions (i.e., Fe^{2+} & Zn^{2+}) bio-adsorbent.

2.3. CNS-AC Characterization

FTIR and SEM were used to analyze the CNS-AC surface. FTIR was used to determine the vibration frequency changes in the functional groups in the biosorbents before and after the biosorption experiments. The spectra of the CNS-AC biosorbents were measured using an

Table 2. Comparison with Other Acids

Property	H_3PO_4	H_2SO_4	HCl	HNO_3
Porosity & Surface Area	High microporosity	Medium	Low	Medium
Functional Groups	Phosphate ($-PO_4^{3-}$)	Sulfonate ($-SO_4^{2-}$)	Chloride (-Cl)	Nitrate ($-NO_3^-$)
Metal Affinity (Zn, Fe)	High	Moderate	Low	Moderate
Corrosiveness	Low	High	High	High
Environmental Safety	High	Moderate	Low	Low
Reusability of Adsorbent	High	Low	Low	Moderate

FTIR spectrometer within the range of 400–4,000 cm^{-1} wavenumber. On the other hand, the surface morphology and metal ion distribution on the biosorbent surface were visualized by SEM. SEM images at suitable magnification and resolution were obtained and interpreted. EDX and AAS analyses were conducted to complement each other for the detection or non-detection of the desired element.

2.4. Biosorption in Bi-Solute System

A multi-solute system was first created. Concentrations of Zn metal used for the Zn-system ranged from 20 to 100 mg/L and 5 to 80 mg/L for the Fe-system. Batch sorption experiments were conducted in a constant-temperature room (25 °C) on a rotary shaker at 100 rpm, using a capped 250 mL conical flask. In the adsorption isotherm tests, 0.6 g of CNS-AC was thoroughly mixed in 150 mL of solution. The initial pH was adjusted to 5, either by H_2SO_4 or NaOH solution, depending on the degree of acidity/alkalinity. Three series of binary Zn–Fe solutions were prepared at Zn:Fe ratios of 1:1.3, 1.7:1, and 1:2.6 and were investigated in the concentration range from 5 to 200 mg/L. In a study conducted by F. Wang *et al.* (2017), a ratio of 1:1 was specified, and Park *et al.* (2016) employed a concentration range from 0 to 320 mg/L. After shaking the flasks for 3 h, the reaction mixtures were filtered, and the filtrate was analyzed for the concentrations of Zn^{2+} and Fe^{2+}, respectively, by AAS. Subsequently, the effect of sorbent doses was tested with initial Zn and Fe concentrations of 200 mg/L at pH 5, while varying the CNS-AC doses from 4–40 g/L. The conical flask was shaken at 25 °C as usual for 5 h, after which Zn^{2+} and Fe^{2+} concentrations were determined by AAS.

3. Results and Discussion

3.1. FTIR Spectroscopy Before and After Sorption

Figure 1a showcases the FTIR spectroscopy results for the CNS-AC biosorbent before its application in the sorption of Zn and Fe. The wavenumbers (in cm^{-1}) are associated with specific molecular vibrations or functional groups present in the biosorbent, while the absorbance values indicate the degree of absorption at each corresponding wavenumber. A remarkably high absorbance of 98.04% at 1,044.53 cm^{-1} potentially indicates the involvement of OH or NH-stretching vibrations. The peak at 603.36 cm^{-1} with an absorbance of 97.12% may be associated with metal-oxygen vibrations or other relevant bonding vibrations in the biosorbent. The high absorbance values at both wavenumbers indicate the prominence of these functional groups in the CNS-AC before any interaction with the two adsorbates. Figure 1b presents the FTIR spectroscopy results for the CNS-AC after its application in the sorption of Zn and Fe.

When the wavenumber is 3,359.24 cm^{-1}, a relatively high absorbance of 69.06% suggests the presence of functional groups associated with hydroxyl (–OH) or amino (–NH) vibrations. The presence of these groups supports metal binding. The peaks at 1,621.76 and 1,364.91 cm^{-1}, with absorbance values of 75.75 and 75.62%, respectively, could be attributed to C=O stretching vibrations and C–H bending vibrations, indicating the involvement of carbonyl and aliphatic groups in the biosorption process. An absorption peak at 1,085.19 cm^{-1} with an absorbance of 75.86% may be indicative of C–O stretching vibrations and suggests the presence of polysaccharides or carbohydrates in the biosorbent. Comparing Figure 1a and 1b, it is evident that the FTIR spectra post-sorption exhibit new peaks and changes in absorbance values, indicating the biosorbent's chemical transformation after interacting with zinc and iron. The peaks in the post-sorption spectrum suggest the involvement of specific functional groups in metal binding. In contrast, the FTIR spectrum before sorption provides a baseline understanding of the biosorbent's initial chemical composition, serving as a reference for identifying alterations after metal interaction. Table 3 compares similar wavelengths observed using other biomass for adsorption.

Peaks around 1,621.76 cm^{-1} correspond to C=O stretching in carboxyl groups, which are key metal-binding sites for Zn^{2+} and Fe^{2+} (F. Wang *et al.*, 2017). Carbonyl (C=O) and lactone groups observed around 1,650 cm^{-1} interact with Zn^{2+} and Fe^{2+} via chelation and complexation mechanisms. Those around 1,000–1,200 cm^{-1} suggest the presence of phosphate or sulfonate groups, which enhance Zn^{2+} and Fe^{2+} affinity.

3.2. SEM Micrograph and EDX Pre- and Post-Sorption

Figure 2a shows a rather loosely packed microstructure with a rough texture. But Figure 2b shows a rather tightly packed microstructure with a smoother texture compared to Figure 2a.

In Table 4, the most abundant element in the biosorbent appears to be C with an atomic concentration of 80.07% and a weight concentration of 74.07%. Nitrogen follows with an atomic concentration of 16.59% and a weight concentration of 17.89%. Other elements present in lower concentrations include S, K, Na, Al, Si, P, Mg, Cl, Ca, and Ti. Notably, Fe seemed to have zero atomic and weight concentrations in CNS before metal sorption, as shown in Table 4, due to its elimination by pyrolysis and H_3PO_4 activation. If Fe or Zn is embedded inside the CNS structure, it may not be detected by an EDX machine unless the sample is properly prepared. Saha *et al.* (2016) also reported that Ni was below the detection limit of X-ray

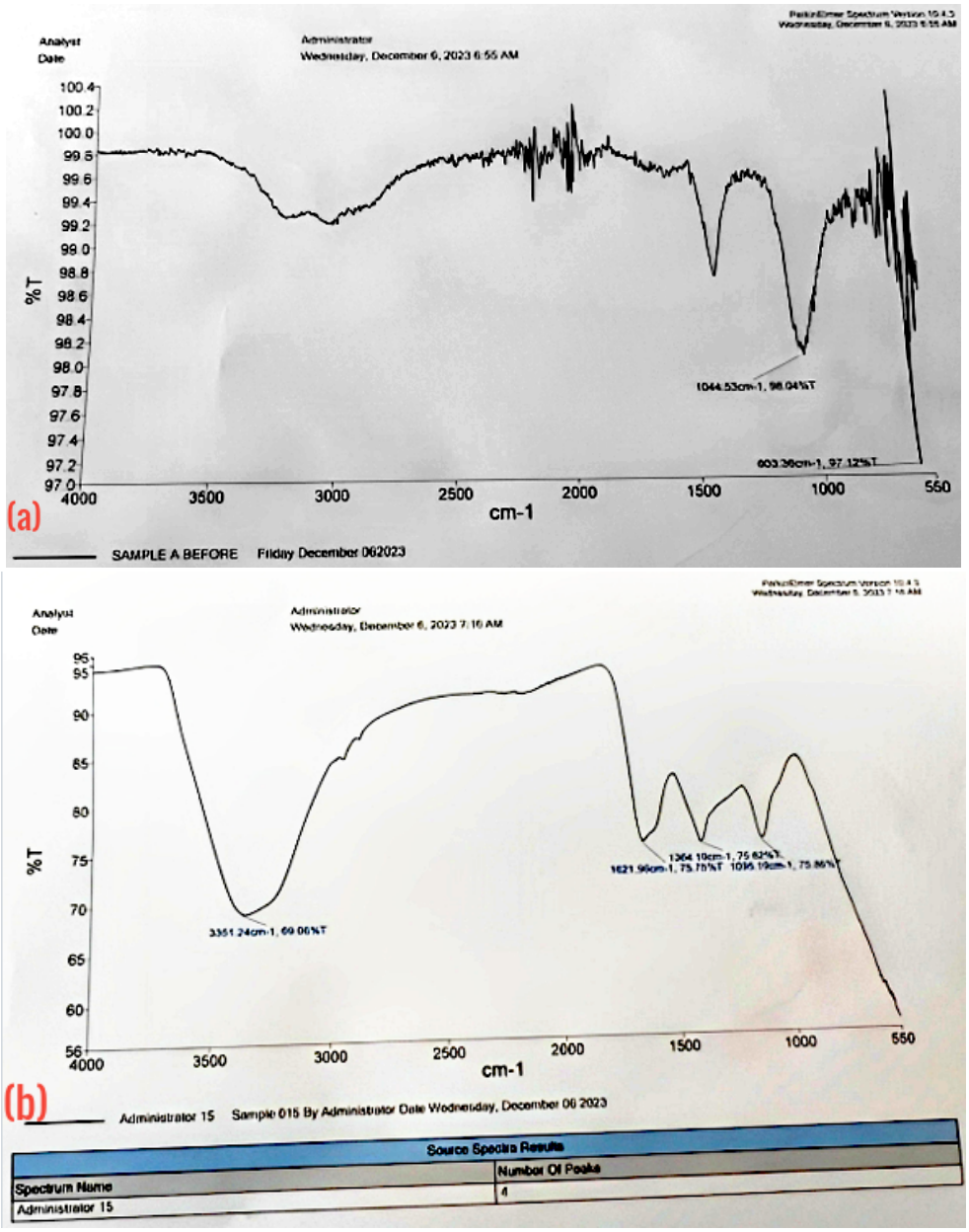

Figure 1. FTIR of CNS-AC Surface (a) Before and (b) After Adsorption

photoelectron spectroscopy, prompting the use of EDX. EDX mainly analyzes the surface layer (a few micrometers deep), and a very low concentration is not sensitive enough. After the Zn-Fe free CNS adsorbent was analyzed after adsorption using an EDX machine, a negligible amount of Fe and Zn was recorded, which is rounded to 0.

Interestingly, upon AAS analysis after sorption, the concentrations of Zn and Fe were obtained and used to calculate the RE of individual and combined metals (co-ion) effects. Notably, after adsorption, C remains the dominant element in the biosorbent even after the metal sorption process, with atomic and weight concentrations of 93.32 and 88.90%, respectively. The variations in the concentrations of other elements become apparent after metal sorption. N, Na, and Cl show noticeable increases, suggesting their involvement in the sorption mechanism. The presence of Na and Cl may indicate the formation of ion-exchange sites on the biosorbent's surface. The presence of competing cations such as Ca^{2+} and Mg^{2+} can interfere with Zn^{2+} adsorption.

Table 3. Comparison of FTIR Wavenumbers of Phosphoric Acid-Activated Biomass

Wavelength (cm^{-1}) CNS Biomass	Wavelength (cm^{-1}) Closest Biomass	Functional Group	Attribution	Closest Biomass Match	Author
3,359.24	3,430	–OH or –NH stretching	Hydroxyl/amino vibrations	Date pits	(El-Hendawy, 2006)
1,621.76	1,700	C=O stretching	Carbonyl group	Medlar seeds	(Bennemla *et al.*, 2024)
1,364.91	1,360	C-H bending	Aliphatic group	Sawdust	(Chikri *et al.*, 2024)
1,085.19	1,100	C–O stretching	Polysaccharides/ carbohydrates	Medlar seeds	(Bennemla *et al.*, 2024)
1,044.53	1,050	–OH or –NH stretching	Hydroxyl/amino vibrations	Sawdust	(Chikri *et al.*, 2024)
603.36	600	Metal–oxygen vibration	Adsorbent-metal interaction	Date pits	(El-Hendawy, 2006)

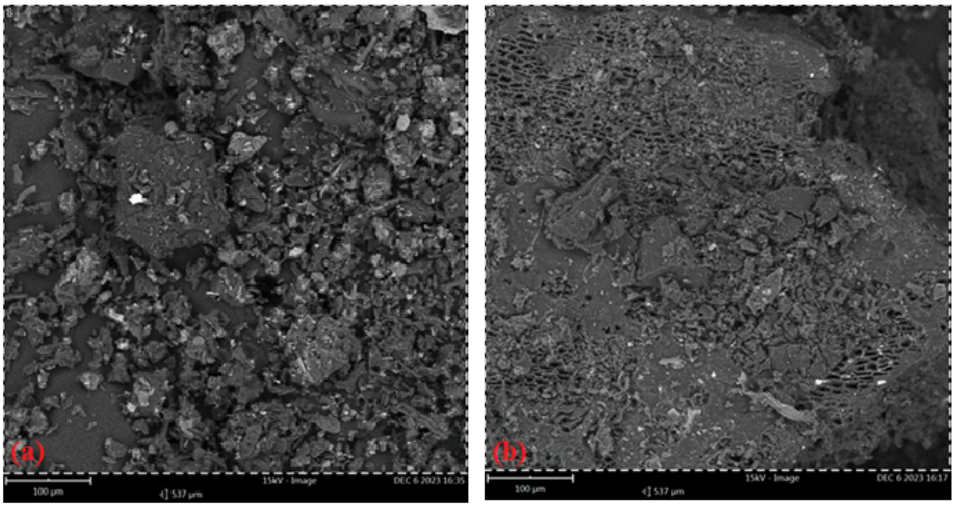

Figure 2. SEM Micrograph of CNS-AC (a) Before and (b) After Sorption

3.3. Effect of Change in the Zn-Fe Initial Concentration

In order to ascertain the effect of co-ion initial concentration (C_o) on equilibrium metal uptake (q_e) for various Zn-Fe concentration ratios of 1:1.3, 1.7:1, and 1:2.6, several plots were made. In Table 5, the RE for Zn decreases as the concentration of Zn increases, a common trend in adsorption processes. At higher Zn-Fe ratios (viz., 1:2.6), Zn RE% tends to be higher at low concentrations, but this is followed by a similar decline at higher concentrations as the Fe ions compete with Zn ions for adsorption sites. For better Zn removal, lower Fe concentrations (especially in the 1:1.3 ratio) are preferred because the Fe ions interfere less with Zn adsorption.

Fe removal is generally higher at lower concentrations but decreases as Fe competes with Zn for adsorption sites. At higher Fe concentrations (1:2.6 ratio), Fe RE% is slightly higher at low C_o but still decreases significantly at high concentrations due to saturation of adsorption sites. CNS-AC has a stronger affinity for Fe than Zn, as Fe RE is slightly higher across all concentration ranges.

3.3.1. Initial Concentration Effect on RE

Zn RE is directly related to how effectively the adsorbent (CNS-AC) removes Zn from the solution. At a ratio of 1:1.3, as the concentration increases from 5 to 200 mg/L, the Zn RE decreases from 5.66 to 0.14%. Thus, Zn removal decreases at higher concentrations, which is expected as the adsorption sites become saturated and the concentration gradient reduces. Similarly, the Zn RE decreases as the C_o increases, when the ratio is 1.7:1. The trend is slightly lower than for the 1:1.3 ratio, indicating that at this Zn-Fe ratio, the RE for Zn may be somewhat more hindered by

Table 4. EDX of CNS-AC Before and After Sorption

Element Number	Element Symbol	Element Name	Atomic Conc. (%)	Weight Conc. (%)
Before Adsorption				
6	C	Carbon	80.07	74.07
7	N	Nitrogen	16.59	17.89
16	S	Sulfur	1.56	3.84
19	K	Potassium	0.39	1.17
11	Na	Sodium	0.38	0.68
13	Al	Aluminum	0.26	0.54
14	Si	Silicon	0.25	0.53
15	P	Phosphorus	0.13	0.32
12	Mg	Magnesium	0.16	0.30
17	Cl	Chlorine	0.11	0.29
20	Ca	Calcium	0.09	0.27
22	Ti	Titanium	0.02	0.08
After Adsorption				
6	C	Carbon	93.32	88.90
7	N	Nitrogen	3.41	3.79
11	Na	Sodium	1.36	2.48
17	Cl	Chlorine	0.48	1.34
14	Si	Silicon	0.34	0.76
16	S	Sulfur	0.26	0.65
13	Al	Aluminum	0.24	0.52
20	Ca	Calcium	0.16	0.51
12	Mg	Magnesium	0.19	0.38
15	P	Phosphorus	0.13	0.32
19	K	Potassium	0.09	0.28
22	Ti	Titanium	0.02	0.07
26	Fe	Iron	0.00	0.00

the higher Fe content. When the ratio is 1:2.6, we observe that Zn RE is initially slightly higher than the previous ratios at lower concentrations (5 mg/L: 5.76%). However, as shown in Figure 3a, as concentration increases, the RE still decreases, and it reaches 0.14% at 200 mg/L. In Figure 3, there is almost a 100% fit for Zn and Fe single sorption at all ratios.

In Figure 3b, the Fe RE follows a similar decreasing trend as Zn RE across all Zn-Fe ratios. After setting the ratio to 1:1.3, Fe RE starts at 9.10% (at 5 mg/L) and decreases to 0.23% (at 200 mg/L). At low concentrations, Fe adsorption is more efficient, but at high concentrations, competition with Zn reduces Fe RE. There is a slightly lower RE compared to the 1:1.3 ratio (at 1.7:1), which indicates that increasing Zn concentration might slightly reduce Fe adsorption efficiency. In Figure 3b, when the ratio is 1:2.6, the highest Fe RE occurs at lower concentrations, likely due to increased Fe presence in the system, leading to a higher probability of Fe adsorption. Figure 4 shows how the RE of Zn and Fe changes when both metals are present in the solution at different ratios and C_o. When the C_o of one metal is higher, it competes with the other for adsorption sites—which means that the presence of more Zn ions can reduce the adsorption of Fe ions, and vice versa. This was

Table 5. Percent Removal and Adsorption Capacity of the Bimetal System of Different Ratios

Zn:Fe Mixture C_o (mg/L)	Zn RE (%)	Fe RE (%)	(Zn + Fe) RE (%)	q_e for Zn (mg/g)	q_e for Fe (mg/g)
Ratio = 1:1.3					
5	5.66	9.10	7.63	0.0301	0.0653
10	2.82	4.62	3.84	0.0303	0.0658
20	1.41	2.33	1.93	0.0304	0.0660
50	0.56	0.93	0.77	0.0305	0.0661
75	0.37	0.62	0.52	0.0305	0.0661
100	0.28	0.47	0.39	0.0305	0.0662
200	0.14	0.23	0.19	0.0305	0.0662
Ratio = 1.7:1					
5	5.53	8.9	6.80	0.0429	0.0421
10	2.76	4.53	3.43	0.0432	0.0424
20	1.38	2.29	1.72	0.0433	0.0426
50	0.55	0.92	0.69	0.0434	0.0427
75	0.37	0.61	0.46	0.0434	0.0427
100	0.28	0.46	0.34	0.0435	0.0427
200	0.14	0.23	0.17	0.0435	0.0427
Ratio = 1:2.6					
5	5.76	9.27	8.32	0.01947	0.08452
10	2.86	4.69	4.19	0.01961	0.08513
20	1.43	2.36	2.10	0.01968	0.08541
50	0.57	0.95	0.84	0.01971	0.08558
75	0.38	0.63	0.56	0.01972	0.08562
100	0.28	0.47	0.42	0.01973	0.08563
200	0.14	0.24	0.21	0.01973	0.08566

the case during the binary sorption of Cd and Cr using landfill clay by Ghorbel-Abid and Trabelsi-Ayadi (2015).

At low C_o (5–10 mg/L), both Zn and Fe show higher percentage removal because there are enough active sites available for adsorption. However, as the concentration increases, the competition between the two ions becomes stronger, resulting in a lower RE, especially for the metal with a lower affinity for the adsorbent. Based on Figure 4, the best ratio for competitive adsorption is the one where the RE is highest for both Zn and Fe (i.e., 1:2.6). From the trends observed in Figure 5, the different Zn-Fe ratios (1:1.3, 1.7:1, and 1:2.6) influence the adsorption performance. At 1:1.3 in Figure 5a, there is a balanced competition between Zn and Fe, meaning both metals have a fair chance of adsorption. But at 1.7:1 (Figure 5b), Zn is at a higher concentration, which may lead to Zn being preferentially adsorbed. Lastly, Fe is at a higher concentration at 1:2.6, which may lead to Fe dominating the adsorption process in Figure 5c. From the observed results in Figure 5, Fe is more strongly adsorbed, followed by Zn+Fe, than Zn, based on RE.

It occurs at a ratio of 1:2.6 with the highest RE of 9.3%, in the order of Fe > Zn+Fe > Zn. The performance is close. Normally, if Zn shows higher RE at a given ratio, it is more strongly adsorbed at that ratio. If Fe shows higher RE, then Fe is better adsorbed. Then, if Zn+Fe together have high RE, the adsorbent effectively captures both metals.

3.3.2. Initial Concentration Effect on Adsorption Capacity

Ni *et al.* (2019) previously explained the single and binary adsorption of Pb(II) and Cd(II) at varying concentrations

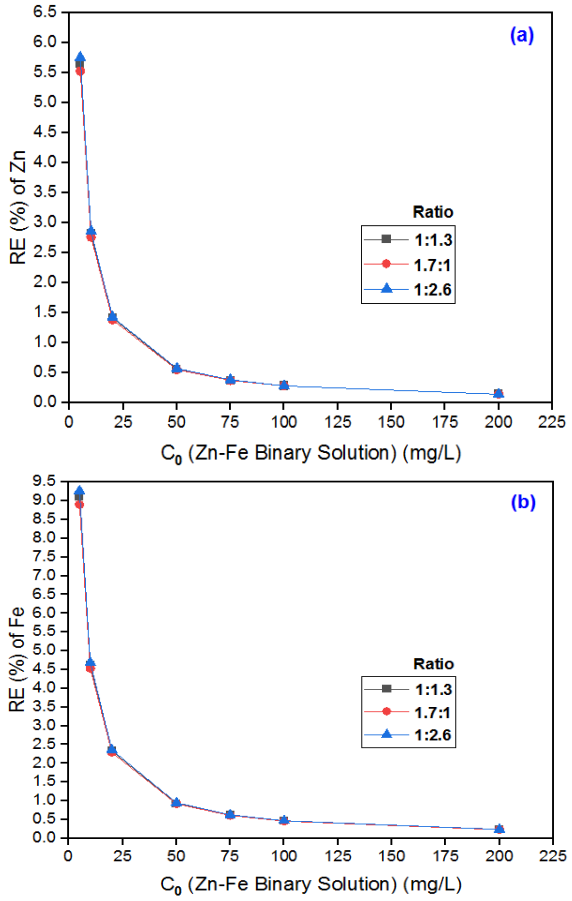

Figure 3. RE Response Influenced by Mono Adsorption of (a) Zn and (b) Fe by CNS-AC from Their Bimetallic Aqueous Solution at Varying Ratio and Initial Concentration

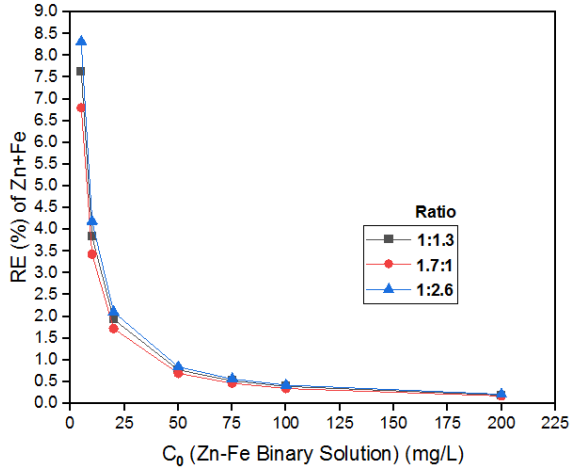

Figure 4. RE Response Influenced by Competitive Adsorption of Zn and Fe at Varying Ratio and Initial Concentration

using sludge biochar. In Figure 6a, which represents Zn mono-adsorption, the uptake increases with an increase in C_o, suggesting that higher Zn concentrations provide a greater driving force for diffusion onto the adsorbent surface. However, at excessively high C_0, the adsorption may reach saturation, leading to a plateau where no

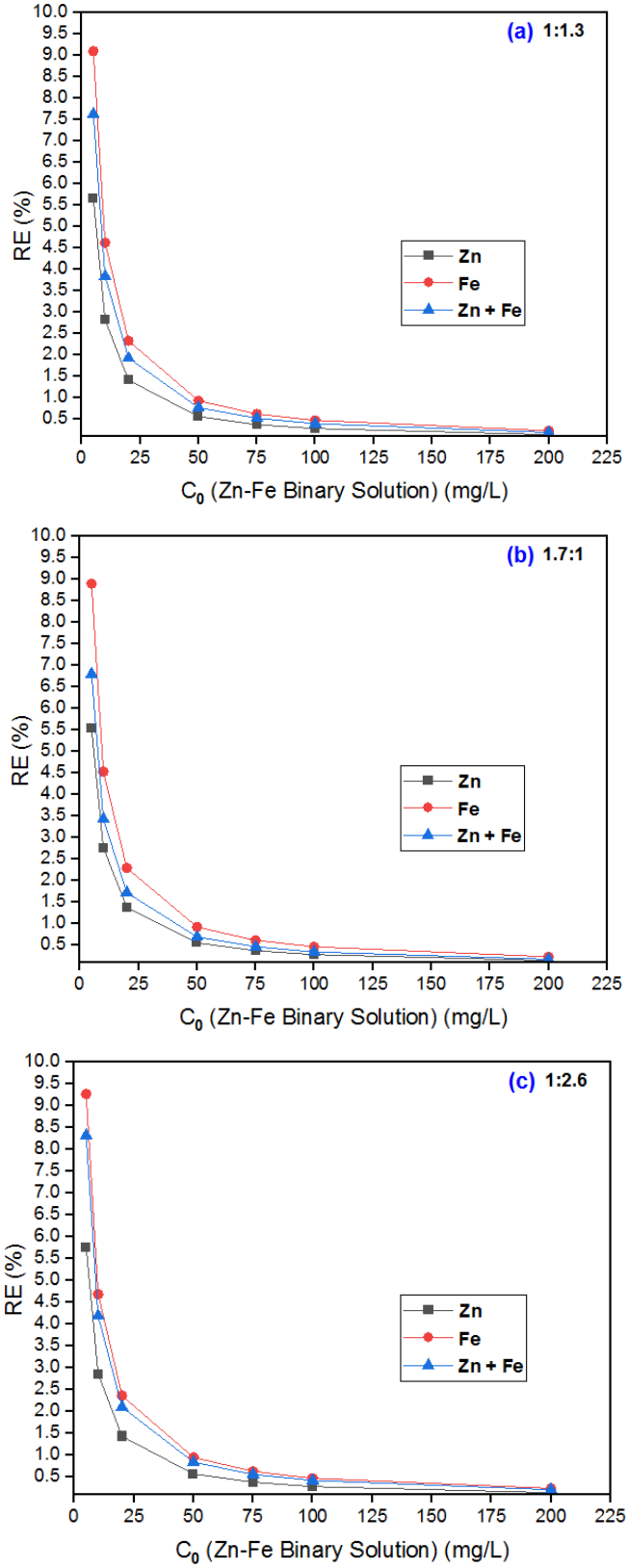

Figure 5. RE Versus Initial Concentration at (a) 1:1.3, (b) 1.7:1, and (c) 1:2.6 Zn-Fe Ratio for Single and Competitive Sorption

significant increase in uptake is observed. The presence of Fe in the bimetallic system likely influences Zn adsorption by competing for available active sites, but since this is mono-adsorption, the interference is minimized. Strongest sorption of Zn occurs at 1.7:1. In comparison, Figure 6a reveals that Zn sorption is highest when the Zn proportion is highest, while Figure 6b shows that Fe adsorption is highest when the Fe proportion is highest in the given ratio.

It is observed that q_e for Fe increases slightly as C_o increases, starting from 0.0653 mg/g at 5 mg/L to 0.0662 mg/g at 200 mg/L when the ratio is 1:1.3 (Figure 6b). Such minimal variation in q_e suggests saturation of active sites at high concentrations. At a ratio of 1.7:1, q_e for Fe increases slightly, from 0.0421 to 0.0427 mg/g within the C_o range. There is a lower q_e compared to the 1:1.3 ratio, indicating that Fe adsorption is hindered when more Zn is present. For 1:2.6, the highest q_e for Fe occurs across all ratios, confirming that Fe has a higher affinity for the adsorbent when at higher concentrations. The results highlight the effectiveness of CNS-AC in removing heavy metals from aqueous solutions and provide insights into optimizing adsorption conditions for selective metal removal. In Figure 7, q_e of both metals against C_o at all ratios depicts a similar trend. The uptake curves for both Zn and Fe increase with C_0 initially in Figure 7a, indicating that more metal ions are available for adsorption. However, as the concentration continues to rise, the curve starts to plateau, suggesting that the adsorbent reaches its saturation point (at 0.03 mg/g for Zn & 0.07 mg/g for Fe). The ratio = 1:1.3 shows a relatively balanced competition between Zn and Fe, leading to moderate adsorption of both metals. Kouakou *et al.* (2013) obtained a q_e = 31 and 15.2 mg/g for Fe and Zn single adsorption using the AC of an unspecified biomass.

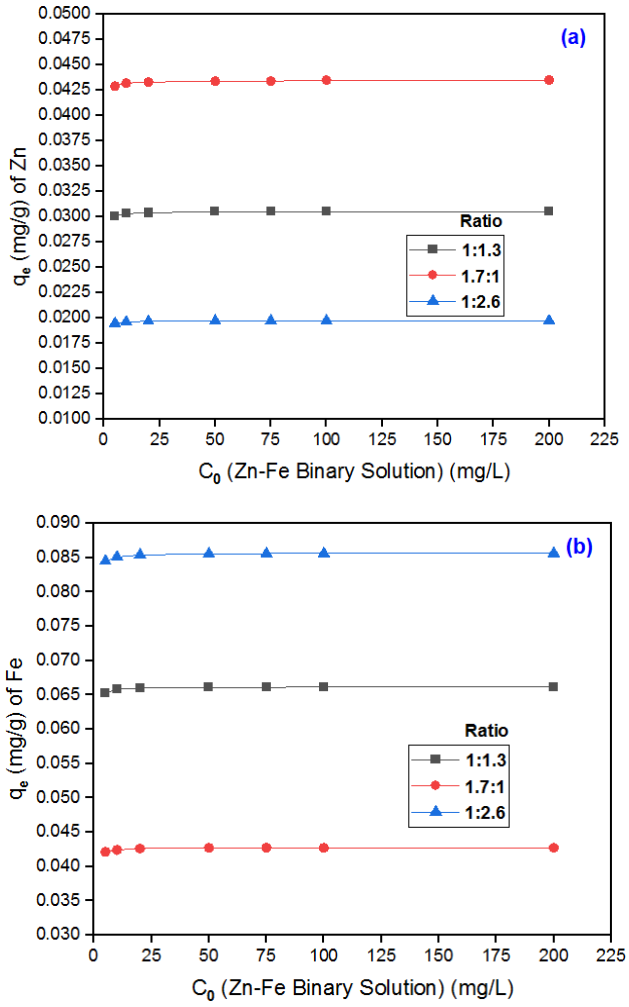

Figure 6. Metal Uptake Response Influenced by Mono Adsorption of (a) Zn and (b) Fe by CNS-AC from Their Bi-Metallic Aqueous Solution at Varying Ratio and C_o

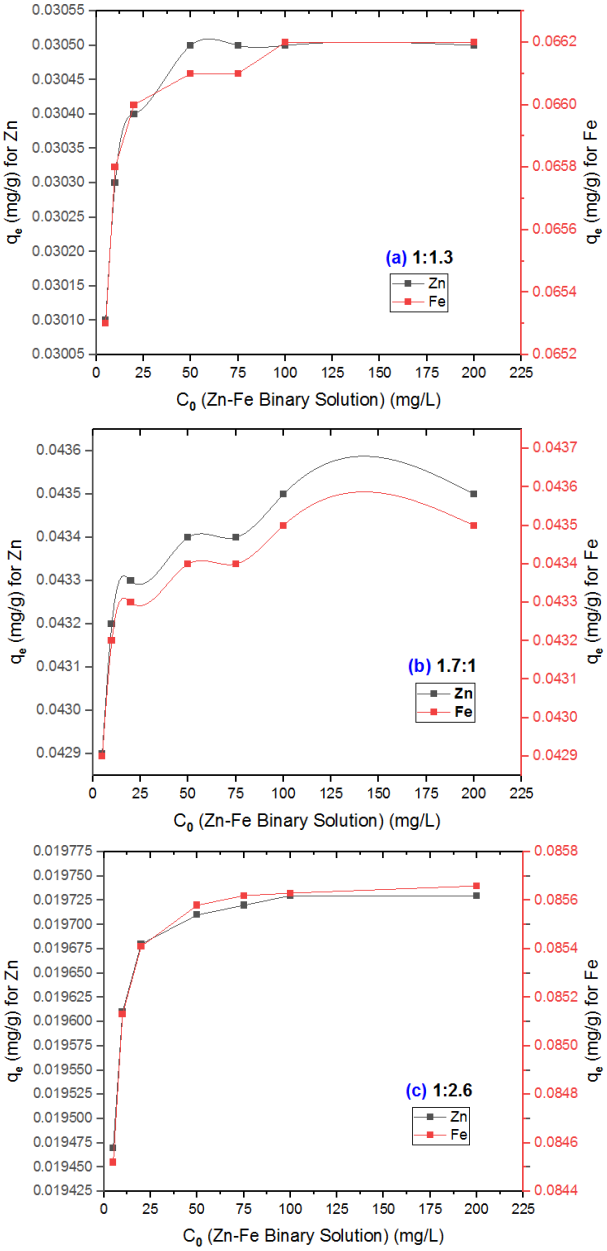

Figure 7. Metal Uptake Versus Initial Concentration at (a) 1:1.3, (b) 1.7:1, and (c) 1:2.6 Zn-Fe Ratio for Single Sorption

In the case of Figure 7b, Zn is in higher proportion relative to Fe (ratio = 1.7:1). As a result, the Zn uptake curve is likely steeper, showing a higher adsorption rate. The Fe uptake curve still increases but at a slower rate, as Zn occupies more of the available active sites. Simply speaking, this suggests that the adsorbent has a preference for Zn at this ratio. As observed in Figure 7c, where the ratio is 1:2.6, Fe is in higher proportion than Zn, which leads to Fe having a stronger adsorption trend. The Fe uptake curve is more pronounced compared to Zn, meaning Fe dominates adsorption (q_e > 0.08 mg/g). Zn uptake is lower due to competition from the higher Fe concentration. Under varying C_o and considering their q_e trend, if the aim is to remove both Zn and Fe efficiently, the 1:1.3 ratio is ideal as it balances adsorption; if Zn removal is the priority, the 1.7:1 ratio should be chosen; and if Fe removal is the focus, the 1:2.6 ratio is the most effective.

3.4. Influence of Biosorbent Dosage Change on Zn-Fe Sorption

At various dosages of CNS-AC adsorbent, the Zn-Fe system was used to remove individual or both metals from

water. Table 6 represents the % removal and q_e at various ratios of the metallic blend. The RE and q_e of CNS-AC vary based on the dose and Zn-Fe ratio. It is observed that the RE values increase with increasing CNS-AC dose, which is expected due to the availability of more active sites for adsorption. The highest RE (~28.97%) is observed at the maximum dose of 40 g/L across all Zn-Fe ratios. However, an RE below 30% suggests moderate adsorption efficiency. Typically, highly effective adsorbents achieve RE values above 80%.

At all doses, the Zn-Fe ratio of 1.7:1 shows slightly higher q_e values for Zn and Fe compared to 1:1.3 and 1:2.6, indicating better adsorption performance. This suggests that the 1.7:1 ratio is the most favorable for adsorption, likely due to better interactions between the metal ions and CNS-AC surface sites. At 40 g/L (optimal dose for adsorption), the highest RE (~28.97%) and highest q_e values for Zn (0.91123 mg/g) and Fe (0.10719 mg/g) are observed at the 1.7:1 Zn-Fe ratio. However, increasing the dose beyond 40 g/L might lead to a plateau effect where additional adsorbent does not significantly increase RE. A system containing Zn, Pb, and Cd showed a boost of q_e > 9.15 mg/g in a study by Lee and Shin (2021), which cannot be compared directly with the current work due to differences in concentration values, dosage, and ratio. Figure 8 shows the RE of Zn+Fe as a function of CNS-AC dose for different Zn:Fe ratios. The curve shape remains similar across all ratios, demonstrating a consistent adsorption mechanism where increasing adsorbent mass enhances RE. The main difference lies in the RE magnitude at a given dose.

The 1.7:1 Zn-Fe ratio appears to be the most efficient in terms of both RE and q_e, likely due to less competition between Zn and Fe ions for adsorption sites. If the goal is to maximize Zn removal, the 1.7:1 ratio is ideal; if Fe removal is the priority, 1:2.6 may perform better at higher doses. Since the p-value is much greater than 0.05 (that is, 0.99998), this indicates that there is no statistically significant difference in the RE between the three Zn:Fe ratios. It confirms that while minor variations exist, the adsorption performance of CNS-AC remains consistent across different Zn:Fe ratios. The analysis of variance (ANOVA) test results show that the F-statistic = 1.50×10^{-5}. The three graphs in Figure 8 depict the q_e of Zn and Fe at varying CNS-AC dosages across different Zn:Fe ratios. A similar trend was presented in Z.-R. Liu *et al.* (2008).

Across all three ratios, the q_e of both Zn and Fe increases as CNS-AC dosage increases. Zn exhibits higher adsorption compared to Fe in all cases, implying a stronger affinity of CNS-AC towards Zn than Fe. At 1:1.3 (Figure 9a), q_e for Zn is higher compared to Fe, with a noticeable

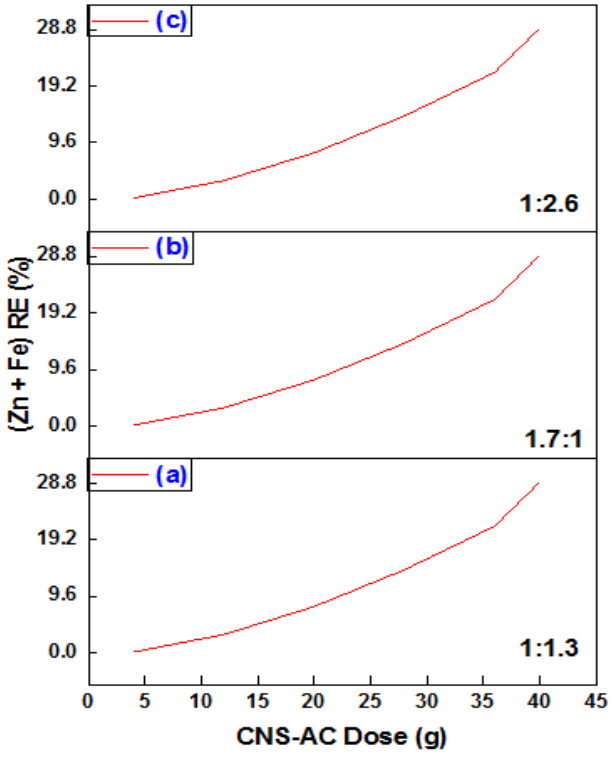

Figure 8. CNS-AC Dosage Impact on REs for Different Ratio Bimetal System

Table 6. RE and Metal Uptakes at Different Ratios by CNS-AC at Various Doses

CNS-AC Dose (g/L)	Zn RE (%)	Fe RE (%)	(Zn + Fe) RE (%)	q_e for Zn (mg/g)	q_e for Fe (mg/g)
Ratio = 1:1.3					
4	0.20	0.20	0.20	0.042032	0.001093
12	3.15	3.15	3.14	0.22776	0.017765
20	7.88	7.88	7.88	0.342037	0.044465
28	14.11	14.10	14.11	0.437752	0.079671
36	21.49	21.49	21.49	0.519065	0.121461
40	28.97	28.97	28.96	0.629578	0.16369
Ratio = 1.7:1					
4	0.17	0.18	0.17	0.05398	0.00062
12	3.13	3.12	3.13	0.3276	0.01155
20	7.85	7.84	7.85	0.49405	0.02905
28	14.08	14.08	14.08	0.63308	0.05212
36	21.48	21.47	21.48	0.75108	0.07951
40	28.95	28.95	28.95	0.91123	0.10719
Ratio = 1:2.6					
4	0.22	0.21	0.22	0.02928	0.00152
12	3.16	3.17	3.17	0.1463	0.02282
20	7.88	7.88	7.88	0.21897	0.05693
28	14.12	14.11	14.11	0.27997	0.10191
36	21.51	21.51	21.51	0.33184	0.1553
40	28.97	28.97	28.98	0.4024	0.20925

increase as CNS-AC dosage increases. The Fe adsorption remains significantly lower but follows a similar increasing trend (0.00109–0.164 mg/g). Secondly, at 1.7:1 (Figure 9b), Zn adsorption remains dominant, with a sharper increase compared to 1:1.3 (0.05398–0.91123 mg/g). The adsorption of Fe also increases but remains relatively low. In Figure 9c for a ratio = 1:2.6, q_e of Fe is more pronounced compared to the other ratios, suggesting that higher Fe concentration in solution enhances its adsorption. However, Zn adsorption is relatively lower than in the 1.7:1 system, indicating competition between the two metals.

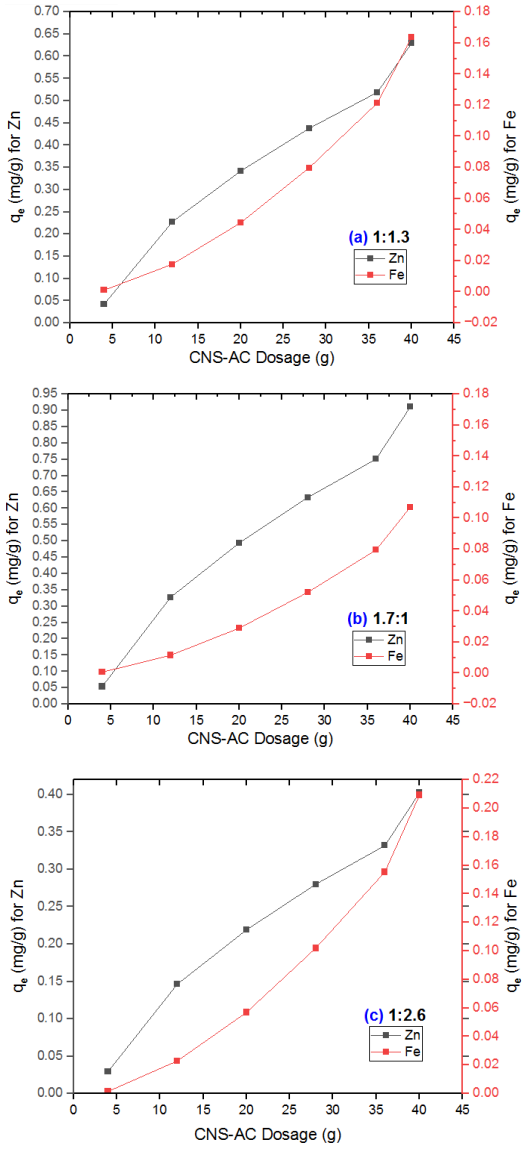

Figure 9. CNS-AC Dosage Correlated with Adsorption Capacity for Different Ratio Bimetal System

4. Conclusion

The current use of H_3PO_4 for activating CNS for adsorbing Zn and Fe is a strategic shift from the use of HCl, H_2SO_4, and HNO_3. A bimetallic solute system at 1:1.3, 1.7:1, and 1:2.6 ratios was formed in this study and was effectively separated into Zn and Fe using CNS. It is observed that competitive sorption exists on the surface of the adsorbent. The affinity of CNS-AC for Zn only, Fe only, or Zn+Fe ions is different at different C_o, dosage, and solute ratio. Findings show that at varying C_o: Zn and Fe have similar uptake values, with no strong preference at 1:1.3; Zn shows the highest uptake since it is in excess at 1.7:1, and Fe exhibits the highest uptake due to its higher proportion at 1:2.6. At varying doses of CNS-AC, highest adsorption (q_e) of Zn and Fe occurs at 1.7:1 and 1:2.6, respectively, against a lower and balanced individual competitive adsorption when the ratio is 1:1.3. AAS gave the concentrations of the ions at various points during the experiment, while FTIR reveals a 1621.76 cm^{-1} C = O stretching vibration that is key to Zn^{2+} and Fe^{2+} binding to CNS-AC adsorbent. Maximum RE of 28.97% occurs at all ratios at a dose = 40 g/L for Zn+Fe removal and 0.19, 0.17, and 0.21% at 200 mg/L C_o at the respective ratios. Given that this is a novel work on adsorbing a Zn-Fe system using any adsorbent, the CNS-AC capability of solving the challenges with HFO, FeO(OH), and iron oxides utilized in the literature for Zn or Fe contamination has been showcased with a moderate

effect. Using CNS-derived AC in this study promotes biowaste valorization and reduces the reliance on synthetic adsorbents. Unlike chemical-based treatments, CNS-AC adsorption does not introduce harmful byproducts, making it an eco-friendly approach. Thermodynamic, isotherm, kinetic, and optimization studies can further be carried out to improve the adsorption capacity of CNS-AC, which recorded a moderate RE in the current study.

References

Abdallah, M. M., Ahmad, M. N., Walker, G., Leahy, J. J., & Kwapinski, W. (2019). Batch and continuous systems for Zn, Cu, and Pb metal ions adsorption on spent mushroom compost biochar. *Industrial & Engineering Chemistry Research*, *58*(17), 7296–7307.

https://doi.org/10.1021/acs.iecr.9b00749

Abdus-Salam, N., & Bello, M. O. (2015). Kinetics, thermodynamics and competitive adsorption of lead and zinc ions onto termite mound. *International Journal of Environmental Science and Technology*, *12*, 3417–3426.

https://doi.org/10.1007/s13762-015-0769-2

Agbenin, J. O., & Olojo, L. A. (2004). Competitive adsorption of copper and zinc by a Bt horizon of a savanna Alfisol as affected by pH and selective removal of hydrous oxides and organic matter. *Geoderma*, *119*(1–2), 85–95.

https://doi.org/10.1016/S0016-7061(03)00242-8

Agwaramgbo, L. O. E., Zulpo, S., & Lira, S. O. (2017). Competitive adsorption of Cu(II) and Zn(II) from binary heavy metal solutions by coffee waste. *British Journal of Applied Science & Technology*, *19*(4), 1–9.

https://doi.org/10.9734/BJAST/2017/31336

Al-Hamandi, H., Aljumaily, M. M., & Al-Obaidi, M. A. (2024). Mono and competitive adsorption of Zn, Cu and Mn in different calcareous soils. *Revista De Agricultura Neotropical*, *11*(3).

https://doi.org/10.32404/rean.v11i3.8543

Azura, A. A., Fauziah, C. I., & Samsuri, A. W. (2012). Cadmium and zinc concentrations in soils and oil palm tissues as affected by long-term application of phosphate rock fertilizers. *Soil and Sediment Contamination: An International Journal*, *21*(5), 586–603.

https://doi.org/10.1080/15320383.2012.672485

Bang, S., Korfiatis, G. P., & Meng, X. (2005). Removal of arsenic from water by zero-valent iron. *Journal of Hazardous Materials*, *121*(1–3), 61–67.

https://doi.org/10.1016/j.jhazmat.2005.01.030

Bashir, A., Manzoor, T., Malik, L. A., Qureashi, A., & Pandith, A. H. (2020). Enhanced and selective adsorption of Zn(II), Pb(II), Cd(II), and Hg(II) ions by a dumbbell- and flower-shaped potato starch phosphate polymer: A combined experimental and DFT calculation study. *ACS Omega*, *5*(10), 4853–4867.

https://doi.org/10.1021/acsomega.9b03607

Benjamin, M. M., & Leckie, J. O. (1981a). Competitive adsorption of Cd, Cu, Zn, and Pb on amorphous iron oxyhydroxide. *Journal of Colloid and Interface Science*, *83*(2), 410–419.

https://doi.org/10.1016/0021-9797(81)90337-4

Benjamin, M. M., & Leckie, J. O. (1981b). Multiple-site adsorption of Cd, Cu, Zn, and Pb on amorphous iron oxyhydroxide. *Journal of Colloid and Interface Science*, *79*(1), 209–221.

https://doi.org/10.1016/0021-9797(81)90063-1

Bennemla, M., Semaoune, T., Sari, M. C., Houhoune, F., Khemaissia, S., Bellaloui, M., Adjedar, H., Hammache, Y., & Ouattas, S. (2024). Preparation and characterization of activated carbon from medlar seed by chemical activation with phosphoric acid and its application in uranium adsorption. *Biomass Conversion and Biorefinery, 15*(9), 14325–14338.

https://doi.org/10.1007/s13399-024-06161-5

Beygi, M., Jalali, M., & Wang, J. (2023). Effect of co-existence of organic acids in the single and competitive adsorption of Cd, Cu, Ni, and Zn to the nanoparticle-treated vineyard soils. *Journal of Soils and Sediments*, *23*, 3043–3059.

https://doi.org/10.1007/s11368-023-03534-7

Bode, K. A. (2023). A comparison of competitive adsorption kinetics between iron, copper, and nickel using soil-based media. Master's thesis. University of Minnesota.

Bouazza, D., Miloudi, H., Adjdir, M., Tayeb, A., & Boos, A. (2018). Competitive adsorption of Cu (II) and Zn (II) on impregnate raw Algerian bentonite and efficiency of extraction. *Applied Clay Science*, *151*, 118–123.

https://doi.org/10.1016/j.clay.2017.10.026

Catts, J. G., & Langmuir, D. (1986). Adsorption of Cu, Pb and Zn by δMnO2: applicability of the site binding-surface complexation model. *Applied Geochemistry*, *1*(2), 255–264.

https://doi.org/10.1016/0883-2927(86)90010-7

Cazanga, M., Gutierrez, M., Escudey, M., Galindo, G., Reyes, A., & Chang, A. C. (2008). Adsorption isotherms of copper, lead, nickel, and zinc in two Chilean soils in single- and multi-component systems: sewage sludge impact on the adsorption isotherms of Diguillin soil. *Australian Journal of Soil Research*, *46*(1), 53–61.

https://doi.org/10.1071/SR07009

Chai, F., Zhang, R., Min, X., Yang, Z., Chai, L., & Zhao, F. (2022). Highly efficient removal of arsenic (III/V) from groundwater using nZVI functionalized cellulose nanocrystals fabricated via a bioinspired strategy. *Science of The Total Environment*, *842*, Article 156937.

https://doi.org/10.1016/j.scitotenv.2022.156937

Chen, G., Yang, L., Chen, J., Miki, T., Li, S., Bai, H., & Nagasaka, T. (2019). Competitive mechanism and influencing factors for the simultaneous removal of Cr(III) and Zn(II) in acidic aqueous solutions using steel slag: Batch and column experiments. *Journal of Cleaner Production*, *230*, 69–79.

https://doi.org/10.1016/j.jclepro.2019.04.402

Chikri, R., Elhadiri, N., Benchanaa, M., & El Maguana, Y. (2024). Two-step optimization of the preparation conditions of a high-quality activated carbon derived from sawdust. *Biomass Conversion and Biorefinery*, *14*, 18151–18164.

https://doi.org/10.1007/s13399-023-03965-9

Choi, J., Septian, A., & Shin, W. S. (2020). The influence of salinity on the removal of Ni and Zn by sorption onto iron oxide- and manganese oxide-coated sand. *Sustainability*, *12,* Article 5815.

https://doi.org/10.3390/su12145815

Choudhury, T. R., Jahan, F. N., Bhowmik, S., Sowrav, S. F. F., & Nurnabi, M. (2024). Enhanced chromium (VI) removal: A remediation study employing nano zero-valent iron supported by sawdust. *Environmental Chemistry and Ecotoxicology*, *6*, 81–91.

https://doi.org/10.1016/j.enceco.2024.02.002

Chubar, N., Carvalho, J. R., & Correia, M. J. N. (2003). Cork biomass as biosorbent for Cu(II), Zn(II) and Ni(II). *Colloids and Surfaces A: Physicochemical and Engineering Aspects*, *230*(1–3), 57–65.

https://doi.org/10.1016/j.colsurfa.2003.09.014

Covelo, E. F., Couce, M. L. A., & Vega, F. A. (2004). Competitive adsorption and desorption of cadmium, chromium, copper, nickel, lead, and zinc by Humic Umbrisols. *Communications in Soil Science and Plant Analysis*, *35*(19–20), 2709–2729.

https://doi.org/10.1081/CSS-200036421

De Oliveira, K. F. S., De Deus Junior, J. O., da Silva do Nascimento, T. L., Dos Anjos, R. B., de Araújo Melo, D. M., Braga, R. M., & de Freitas Melo, M. A. (2021). Cashew nut shell (Anarcadium accidentale L) charcoal as bioadsorbent to remove Cu2+ and Cr3+. *Research, Society and Development*, *10*(2), e0510212238.

https://doi.org/10.33448/rsd-v10i2.12238

Del Rio, M., Escarabajal, J. C. G., Palomino, G. T., & Cabello, C. P. (2022). Zinc/Iron mixed-metal MOF-74 derived magnetic carbon nanorods for the enhanced removal of organic pollutants from water. *Chemical Engineering Journal*, *428*, Article 131147.

https://doi.org/10.1016/j.cej.2021.131147

Depci, T., Kul, A. R., & Önal, Y. (2012). Competitive adsorption of lead and zinc from aqueous solution on activated carbon prepared from Van apple pulp: Study in single- and multi-solute systems. *Chemical Engineering Journal*, *200–202*, 224–236.

https://doi.org/10.1016/j.cej.2012.06.077

Ding, Z., Hu, X., Wan, Y., Wang, S., & Gao, B. (2016). Removal of lead, copper, cadmium, zinc, and nickel from aqueous solutions by alkali-modified biochar: Batch and column tests. *Journal of Industrial and Engineering Chemistry*, *33*, 239–245.

https://doi.org/10.1016/j.jiec.2015.10.007

Du, X., Cui, S., Fang, X., Wang, Q., & Liu, G. (2020). Adsorption of Cd(II), Cu(II), and Zn(II) by granules prepared using sludge from a drinking water purification plant. *Journal of Environmental Chemical Engineering*, *8*(6), Article 104530.

https://doi.org/10.1016/j.jece.2020.104530

Du, X., Cui, S., Wang, Q., Han, Q., & Liu, G. (2021). Non-competitive and competitive adsorption of Zn(II), Cu(II), and Cd(II) by a granular Fe-Mn binary oxide in aqueous solution. *Environmental Progress & Sustainable Energy*, *40*(4), e13611.

https://doi.org/10.1002/ep.13611

Ebrahim, S. E., Sulaymon, A. H., & Alhares, H. S. (2016). Competitive removal of Cu2+, Cd2+, Zn2+, and Ni2+ ions onto iron oxide nanoparticles from wastewater. *Desalination and Water Treatment*, *57*(44), 20915–20929.

https://doi.org/10.1080/19443994.2015.1112310

Ebrahime, S. E., & Alsaade, S. H. (2019). Competitive adsorption of Cd (II) and Zn (II) in single and binary systems from aqueous solutions onto cork stopper particles. *Association of Arab Universities Journal of Engineering Sciences*, *26*(1), 17–27.

https://doi.org/10.33261/jaaru.2019.26.1.003

Edward, D., Karungamye, P., Nelson, G., Selemani, J., & Njau, K. N. (2023). Removal of arsenic in a sand filter coupled with zero valent iron. *HydroResearch*, *6*, 228–234.

https://doi.org/10.1016/j.hydres.2023.06.002

Einhorn, V., Haase, H., & Maares, M. (2024). Interaction and competition for intestinal absorption by zinc, iron, copper, and manganese at the intestinal mucus layer. *Journal of Trace Elements in Medicine and Biology*, *84*, Article 127459, 1–10.

https://doi.org/10.1016/j.jtemb.2024.127459

El-Hendawy, A.-N. A. (2006). Variation in the FTIR spectra of a biomass under impregnation, carbonization and oxidation conditions. *Journal of Analytical and Applied Pyrolysis*, *75*(2), 159–166.

https://doi.org/10.1016/j.jaap.2005.05.004

Eloussaief, M., Hamza, W., Kallel, N., & Benzina, M. (2013). Wastewaters decontamination: Mechanisms of Pb(II), Zn(II), and Cd(II) competitive adsorption on tunisian smectite in single and multi-solute systems. *Environmental Progress & Sustainable Energy*, *32*(2), 229–238.

https://doi.org/10.1002/ep.11609

Esfandiar, N., Suri, R., & McKenzie, E. R. (2022). Competitive sorption of Cd, Cr, Cu, Ni, Pb and Zn from stormwater runoff by five low-cost sorbents; Effects of co-contaminants, humic acid, salinity and pH. *Journal of Hazardous Materials*, *423*, Article 126938, 1–13.

https://doi.org/10.1016/j.jhazmat.2021.126938

Fernández-Calviño, D., Pérez-Novo, C., Bermúdez-Couso, A., López-Periago, E., & Arias-Estévez, M. (2010). Batch and stirred flow reactor experiments on Zn sorption in acid soils: Cu competition. *Geoderma*, *159*(3–4), 417–424.

https://doi.org/10.1016/j.geoderma.2010.09.007

Fontes, M. P. F., De Matos, A. T., Da Costa, L. M., & Neves, J. C. L. (2000). Competitive adsorption of zinc, cadmium, copper, and lead in three highly-weathered Brazilian soils. *Communications in Soil Science and Plant Analysis*, *31*(17–18), 2939–2958.

https://doi.org/10.1080/00103620009370640

Fungaro, D. A., & Graciano, J. E. A. (2007). Adsorption of zinc ions from water using zeolite/iron oxide composites. *Adsorption Science & Technology*, *25*(10), 729–740.

https://doi.org/10.1260/026361707785284185

Gabaldón, C., Marzal, P., Ferrer, J., & Seco, A. (1996). Single and competitive adsorption of Cd and Zn onto a granular activated carbon. *Water Research*, *30*(12), 3050–3060.

https://doi.org/10.1016/S0043-1354(96)00165-0

García-Mendieta, A., Olguín, M. T., & Solache-Ríos, M. (2012). Biosorption properties of green tomato husk (Physalis philadelphica Lam) for iron, manganese and iron–manganese from aqueous systems. *Desalination*, *284*, 167–174.

https://doi.org/10.1016/j.desal.2011.08.052

Garrido-Rodriguez, B., Cutillas-Barreiro, L., Fernández-Calviño, D., Arias-Estévez, M., Fernández-Sanjurjo, M. J., Álvarez-Rodríguez, E., & Núñez-Delgado, A. (2014). Competitive adsorption and transport of Cd, Cu, Ni and Zn in a mine soil amended with mussel shell. *Chemosphere*, *107*, 379–385.

https://doi.org/10.1016/j.chemosphere.2013.12.097

Ghorbel-Abid, I., & Trabelsi-Ayadi, M. (2015). Competitive adsorption of heavy metals on local landfill clay. *Arabian Journal of Chemistry*, *8*, 25–31.

https://doi.org/10.1016/j.arabjc.2011.02.030

Gibert, O., Abenza, M., Reig, M., Vecino, X., Sánchez, D., Arnaldos, M., & Cortina, J. L. (2022). Removal of nitrate from groundwater by nano-scale zero-valent iron injection pulses in continuous-flow packed soil columns. *Science of The Total Environment*, *810*, Article 152300, 1–10.

https://doi.org/10.1016/j.scitotenv.2021.152300

Giles, D. E., Mohapatra, M., Issa, T. B., Anand, S., & Singh, P. (2011). Iron and aluminium based adsorption strategies for removing arsenic from water. *Journal of Environmental Management*, *92*(12), 3011–3022.

https://doi.org/10.1016/j.jenvman.2011.07.018

Gu, X., & Evans, L. J. (2007). Modelling the adsorption of Cd(II), Cu(II), Ni(II), Pb(II), and Zn(II) onto Fithian illite. *Journal of Colloid and Interface Science*, *307*(2), 317–325.

https://doi.org/10.1016/j.jcis.2006.11.022

Gu, X., & Evans, L. J. (2008). Surface complexation modelling of Cd(II), Cu(II), Ni(II), Pb(II) and Zn(II) adsorption onto kaolinite. *Geochimica et Cosmochimica Acta*, *72*(2), 267–276.

https://doi.org/10.1016/j.gca.2007.09.032

Guijarro-Aldaco, A., Hernández-Montoya, V., Bonilla-Petriciolet, A., Montes-Morán, M. A., & Mendoza-Castillo, D. I. (2011). Improving the adsorption of heavy metals from water using commercial carbons modified with egg shell wastes. *Industrial & Engineering Chemistry Research*, *50*(15), 9354–9362.

https://doi.org/10.1021/ie2006627

Guo, S., Dan, Z., Duan, N., Chen, G., Gao, W., & Zhao, W. (2018). Zn(II), Pb(II), and Cd(II) adsorption from aqueous solution by magnetic silica gel: preparation, characterization, and adsorption. *Environmental Science and Pollution Research*, *25*, 30938–30948.

https://doi.org/10.1007/s11356-018-3050-7

Guo, S., Jiao, P., Dan, Z., Duan, N., Zhang, J., Chen, G., & Gao, W. (2017). Synthesis of magnetic bioadsorbent for adsorption of Zn(II), Cd(II) and Pb(II) ions from aqueous solution. *Chemical Engineering Research and Design*, *126*, 217–231.

https://doi.org/10.1016/j.cherd.2017.08.025

Hafshejani, L. D., Nasab, S. B., Shirazi, P., Hafshejani, S. B., & Gholami, R. M. (2015). Competitive effects of iron, zinc, and cadmium ions on lead removal from aqueous solutions using the nanostructured ash cedar absorbent. *Journal of Water and Wastewater*, *26*(3), 11–18. https://www.wwjournal.ir/article_7842.html?lang=en

Han, J.-G., Kim, D.-C., Hong, K.-K., & Yoon, W.-I. (2012). Competive adsorption characteristics of CFW on Cu and Zn. *Journal of the Korean Geosynthetics Society*, *11*(1), 1–9.

https://doi.org/10.12814/jkgss.2012.11.1.001

Helios-Rybicka, E., & Wójcik, R. (2012). Competitive sorption/desorption of Zn, Cd, Pb, Ni, Cu, and Cr by clay-bearing mining wastes. *Applied Clay Science*, *65–66*, 6–13.

https://doi.org/10.1016/j.clay.2012.06.006

Hong, G., Shan, R., Gu, J., Huhe, T., Yuan, H., & Chen, Y. (2024). Fe-Zn bimetallic oxide functionalized biochar for enhanced adsorption of enrofloxacin in water. *Journal of Environmental Chemical Engineering*, *12*(2), Article 112208.

https://doi.org/10.1016/j.jece.2024.112208

Ighalo, J. O., Adeniyi, A. G., Eletta, O. A. A., & Arowoyele, L. T. (2020). Competitive adsorption of Pb(II), Cu(II), Fe(II) and Zn(II) from aqueous media using biochar from oil palm (Elaeis guineensis) fibers: a kinetic and equilibrium study. *Indian Chemical Engineer*, *63*(5), 501–511.

https://doi.org/10.1080/00194506.2020.1787870

Islam, M. A., Nazal, M. K., Angove, M. J., Morton, D. W., Hoque, K. A., Reaz, A. H., Islam, M. T., Abdul Karim, S. M., & Chowdhury, A.-N. (2024). Emerging iron-based mesoporous materials for adsorptive removal of pollutants: Mechanism, optimization, challenges, and future perspective. *Chemosphere*, *349*, Article 140846.

https://doi.org/10.1016/j.chemosphere.2023.140846

Jalali, M., & Moradi, F. (2013). Competitive sorption of Cd, Cu, Mn, Ni, Pb and Zn in polluted and unpolluted calcareous soils. *Environmental Monitoring and Assessment*, *185*, 8831–8846.

https://doi.org/10.1007/s10661-013-3216-1

Jalali, M., Ragheb, S. B., & Moharami, S. (2024). Mono and competitive adsorption-desorption of Cd, Co, Cu, and Zn in ten agricultural and greenhouse soils. *Soil and Sediment Contamination: An International Journal*, *33*(7), 976–999.

https://doi.org/10.1080/15320383.2023.2283121

Jiang, K., Liu, K., Peng, Q., & Zhou, M. (2021). Adsorption of Pb(II) and Zn(II) ions on humus-like substances modified montmorillonite. *Colloids and Surfaces A: Physicochemical and Engineering Aspects*, *631*, Article 127706.

https://doi.org/10.1016/j.colsurfa.2021.127706

Joseph, I. V, Tosheva, L., & Doyle, A. M. (2020). Simultaneous removal of Cd(II), Co(II), Cu(II), Pb(II), and Zn(II) ions from aqueous solutions via adsorption on FAU-type zeolites prepared from coal fly ash. *Journal of Environmental Chemical Engineering*, *8*(4).

https://doi.org/10.1016/j.jece.2020.103895

Kalbasi, M., Racz, G. J., & Loewen-Rudgers, L. A. (1978). Mechanism of zinc adsorption by iron and aluminum oxides. *Soil Science*, *125*(3), 146–150. https://journals.lww.com/soilsci/abstract/1978/03000

Kanel, S. R., Manning, B., Charlet, L., & Choi, H. (2005). Removal of arsenic(III) from groundwater by nanoscale zero-valent iron. *Environmental Science & Technology*, *39*(5), 1291–1298.

https://doi.org/10.1021/es048991u

Kanungo, S. B. (1994). Adsorption of cations on hydrous oxides of iron: III. adsorption of Mn, Co, Ni, and Zn on βFeOOH from simple electrolyte solutions as well as from a complex electrolyte solution resembling seawater in major ion content. *Journal of Colloid and Interface Science*, *162*(1), 103–109.

https://doi.org/10.1006/jcis.1994.1014

Kanungo, S. B., Tripathy, S. S., & Rajeev. (2004). Adsorption of Co, Ni, Cu, and Zn on hydrous manganese dioxide from complex electrolyte solutions resembling sea water in major ion content. *Journal of Colloid and Interface Science*, *269*(1), 1–10.

https://doi.org/10.1016/S0021-9797(03)00464-8

Kinniburgh, D. G., & Jackson, M. L. (1982). Concentration and pH dependence of calcium and zinc adsorption by iron hydrous oxide gel. *Soil Science Society of America Journal*, *46*(1), 56–61.

https://doi.org/10.2136/sssaj1982.03615995004600010010x

Kouakou, U., Ello, A. S., Yapo, J. A., & Trokourey, A. (2013). Adsorption of iron and zinc on commercial activated carbon. *Journal of Environmental Chemistry and Ecotoxicology*, *5*(6), 168–171.

https://doi.org/10.5897/JECE2013.0264

Krok, B., Mohammadian, S., Noll, H. M., Surau, C., Markwort, S., Fritzsche, A., Nachev, M., Sures, B., & Meckenstock, R. U. (2022). Remediation of zinc-contaminated groundwater by iron oxide in situ adsorption barriers – From lab to the field. *Science of The Total Environment*, *807*(3), 1–12.

https://doi.org/10.1016/j.scitotenv.2021.151066

Kumar, P. S., Ramalingam, S., Abhinaya, R. V., Kirupha, S. D., Vidhyadevi, T., & Sivanesan, S. (2012). Adsorption equilibrium, thermodynamics, kinetics, mechanism and process design of zinc (II) ions onto cashew nut shell. *The Canadian Journal of Chemical Engineering*, *90*, 973–982.

https://doi.org/10.1002/cjce.20588

Kumar, P. S., Ramalingam, S., Abhinaya, R. V., Thiruvengadaravi, K. V., Baskaralingam, P., & Sivanesan, S. (2011). Lead (II) adsorption onto sulphuric acid treated cashew nut shell. *Separation Science and Technology*, *46*(15), 2436–2449.

https://doi.org/10.1080/01496395.2011.590174

Kumar, P. S., Ramalingam, S., Kirupha, S. D., Murugesan, A., Vidhyadevi, T., & Sivanesan, S. (2011). Adsorption behavior of nickel(II) onto cashew nut shell: Equilibrium, thermodynamics, kinetics, mechanism and process design. *Chemical Engineering Journal*, *167*(1), 122–131.

https://doi.org/10.1016/j.cej.2010.12.010

Kummer, L., Gonçalves, M. S., Zemiani, A., de Freitas Melo, V., & Gomes, S. D. (2018). Individual and competitive adsorption of copper, zinc and lead in soils with contrasting texture. *Journal of Experimental Agriculture International*, *27*(1), 1–11.

https://doi.org/10.9734/JEAI/2018/43891

Lee, H.-S., & Shin, H.-S. (2021). Competitive adsorption of heavy metals onto modified biochars: Comparison of biochar properties and modification methods. *Journal of Environmental Management*, *299*, Article 113651.

https://doi.org/10.1016/j.jenvman.2021.113651

Li, M., Li, M., Feng, C., & Zeng, Q. (2014). Preparation and characterization of multi-carboxyl-functionalized silica gel for removal of Cu (II), Cd (II), Ni (II) and Zn (II) from aqueous solution. *Applied Surface Science*, *314*, 1063–1069.

https://doi.org/10.1016/j.apsusc.2014.06.038

Li, Y. W., Zhao, B. W., Wang, L., Li, Y. Q., Wang, T., Jia, Y. H., & Zhao, M. L. (2024). Competitive adsorption of Cd(II) and Zn(II) on biochar, loess, and biocharloess mixture. *Nature Environment and Pollution Technology*, *23*(1), 265–273.

https://doi.org/10.46488/NEPT.2024.v23i01.022

Liu, C.-C., Wang, M.-K., Chiou, C.-S., Li, Y.-S., Yang, C.-Y., & Lin, Y.-A. (2009). Biosorption of chromium, copper and zinc by wine-processing waste sludge: Single and multi-component system study. *Journal of Hazardous Materials*, *171*(1–3), 386–392.

https://doi.org/10.1016/j.jhazmat.2009.06.012

Liu, H., Wang, C., Liu, J., Wang, B., & Sun, H. (2013). Competitive adsorption of Cd(II), Zn(II) and Ni(II) from their binary and ternary acidic systems using tourmaline. *Journal of Environmental Management*, *128*, 727–734.

https://doi.org/10.1016/j.jenvman.2013.06.024

Liu, Z.-R., Zhou, L.-M., Wei, P., Zeng, K., Wen, C.-X., & Lan, H.-H. (2008). Competitive adsorption of heavy metal ions on peat. *Journal of China University of Mining and Technology*, *18*(2), 255–260.

https://doi.org/10.1016/S1006-1266(08)60054-1

Lu, M., Zhang, Y., Su, Z., Liu, S., Liu, J., & Jiang, T. (2021). Mechanisms and model study of Zn(II) and Cd(II) competitive adsorption on V, Ti-bearing magnetite-humic acid adsorbent. *Desalination and Water Treatment*, *224*, 308–321.

https://doi.org/10.5004/dwt.2021.27195

Lu, S. G., & Xu, Q. F. (2009). Competitive adsorption of Cd, Cu, Pb and Zn by different soils of Eastern China. *Environmental Geology*, *57*, 685–693.

https://doi.org/10.1007/s00254-008-1347-4

Luka, Y., Chiroma, T. M., Abubakar, A. M., & Kachalla, A. D. (2024). Zinc adsorption from synthetic wastewater using synthesized activated carbons from sugarcane bagasse and cashew nut shells before determination by atomic absorption spectrometry. *Analytical Methods in Environmental Chemistry Journal (AMECJ)*, *7*(4), 78–95.

https://doi.org/10.24200/amecj.v7.i04.345

Lv, X., Peng, H., Wang, X., Hu, L., Peng, M., Liu, Z., & Jiang, G. (2022). Nitrate reduction by nanoscale zero valent iron (nFe0)-based Systems: Mechanism, reaction pathway and strategy for enhanced N2 formation. *Chemical Engineering Journal*, *430*(Part 4).

https://doi.org/10.1016/j.cej.2021.133133

Madrid, L., Diaz-Barrientos, E., & Contreras, M. C. (1991). Relationships between zinc and phosphate adsorption on montmorillonite and an iron oxyhydroxide. *Australian Journal of Soil Research*, *29*(2), 239–247.

https://doi.org/10.1071/SR9910239

Mahamadi, C., & Nharingo, T. (2010). Competitive adsorption of Pb2+, Cd2+ and Zn2+ ions onto Eichhornia crassipes in binary and ternary systems. *Bioresource Technology*, *101*(3), 859–864.

https://doi.org/10.1016/j.biortech.2009.08.097

Mesquita, M. E., & Carranca, C. (2005). Effect of dissolved organic matter on copper-zinc competitive adsorption by a sandy soil at different pH values. *Environmental Technology*, *26*(9), 1065–1072.

https://doi.org/10.1080/09593332608618493

Mesquita, M. E., Carranca, C., & Menino, M. R. (2002). Influence of pH on copper-zinc competitive adsorption by a sandy soil. *Environmental Technology*, *23*(9), 1043–1050.

https://doi.org/10.1080/09593332308618352

Mesquita, M. E., & e Silva, J. M. V. (2002). Preliminary study of pH effect in the application of Langmuir and Freundlich isotherms to Cu–Zn competitive adsorption. *Geoderma*, *106*(3–4), 219–234.

https://doi.org/10.1016/S0016-7061(01)00125-2

Mesquita, M. E., Silva, J. M. V. E., Branco, M. A. C., & Sequeira, E. M. (2000). Copper and zinc competitive adsorption: Desorption in calcareous soils. *Arid Soil Research and Rehabilitation*, *14*(1), 27–41.

https://doi.org/10.1080/089030600263157

Mihajlović, M. T., Lazarević, S. S., Janković-Častvan, I. M., Kovač, J., Jokić, B. M., Janaćković, D. T., & Petrović, R. D. (2015). Kinetics, thermodynamics, and structural investigations on the removal of Pb2+, Cd2+, and Zn2+ from multicomponent solutions onto natural and Fe(III)-modified zeolites. *Clean Technologies and Environmental Policy*, *17*, 407–419.

https://doi.org/10.1007/s10098-014-0794-8

Millward, G. E., & Moore, R. M. (1982). The adsorption of Cu, Mn and Zn by iron oxyhydroxide in model estuarine solutions. *Water Research*, *16*(6), 981–985.

https://doi.org/10.1016/0043-1354(82)90032-X

Ming, H., Naidu, R., Sarkar, B., Lamb, D. T., Liu, Y., Megharaj, M., & Sparks, D. (2016). Competitive sorption of cadmium and zinc in contrasting soils. *Geoderma*, *268*, 60–68.

https://doi.org/10.1016/j.geoderma.2016.01.021

Mo, W., He, C., Yang, Y., Cheng, B., Yang, J., & Huang, Y. (2024). Adsorption behavior of Mg–Al layered double hydroxide on Pb(II), Zn(II), Cd(II), and As(V) coexisting in aqueous

solution. *Materials Today Sustainability*, *27*, Article 100861.

https://doi.org/10.1016/j.mtsust.2024.100861

Mohammadi, R., Azadmehr, A., & Maghsoudi, A. (2019). Fabrication of the alginate-combusted coal gangue composite for simultaneous and effective adsorption of Zn(II) and Mn(II). *Journal of Environmental Chemical Engineering*, *7*(6).

https://doi.org/10.1016/j.jece.2019.103494

Mohammadi, R., Azadmehr, A., & Maghsoudi, A. (2020). Enhancing of competitive adsorptive removal of zinc and manganese from aqueous solution by iron oxide-combusted coal gangue composite. *Separation Science and Technology*, *55*(18), 3343–3361.

https://doi.org/10.1080/01496395.2019.1706570

Mohammadi, R., Azadmehr, A., & Maghsoudi, A. (2021). Enhanced competitive adsorption of zinc and manganese by alginate-iron oxide-combusted coal gangue composite: Synthesizing, characterization and investigation. *Journal of Environmental Chemical Engineering*, *9*(1).

https://doi.org/10.1016/j.jece.2020.105003

Mohan, D., & Chander, S. (2006). Single, binary, and multicomponent sorption of iron and manganese on lignite. *Journal of Colloid and Interface Science*, *299*(1), 76–87.

https://doi.org/10.1016/j.jcis.2006.02.010

Moreira, C. S., & Alleoni, L. R. F. (2010). Adsorption of Cd, Cu, Ni and Zn in tropical soils under competitive and non-competitive systems. *Scientia Agricola*, *67*(3), 301–307.

https://doi.org/10.1590/S0103-90162010000300008

Muhammad, Chuah, T. G., Robiah, Y., Suraya, A. R., & Choong, T. S. Y. (2011). Single and binary adsorptions isotherms of Cd(II) and Zn(II) on palm kernel shell based activated carbon. *Desalination and Water Treatment*, *29*(1–3), 140–148.

https://doi.org/10.5004/dwt.2011.2210

Musić, S., & Ristic, M. (1992). Adsorption of zinc(II) on hydrous iron oxides. *Journal of Radioanalytical and Nuclear Chemistry*, *162*, 351–362.

https://doi.org/10.1007/BF02035395

Nguyen, T. C., Loganathan, P., Nguyen, T. V., Vigneswaran, S., Kandasamy, J., & Naidu, R. (2015). Simultaneous adsorption of Cd, Cr, Cu, Pb, and Zn by an iron-coated Australian zeolite in batch and fixed-bed column studies. *Chemical Engineering Journal*, *270*, 393–404.

https://doi.org/10.1016/j.cej.2015.02.047

Ni, B.-J., Huang, Q.-S., Wang, C., Ni, T.-Y., Sun, J., & Wei, W. (2019). Competitive adsorption of heavy metals in aqueous solution onto biochar derived from anaerobically digested sludge. *Chemosphere*, *219*, 351–357.

https://doi.org/10.1016/j.chemosphere.2018.12.053

Niu, Z., Xue, Q., Qi, S., Guo, Y., & Chen, H. (2018). Effect of multifactors interaction on competitive adsorption of Zn2+ and Cd2+ by response surface methodology. *Environmental Earth Sciences*, *77*(244).

https://doi.org/10.1007/s12665-018-7426-2

Oladipo, A. A., Ahaka, E. O., & Gazi, M. (2019). High adsorptive potential of calcined magnetic biochar derived from banana peels for Cu2+, Hg2+, and Zn2+ ions removal in single and ternary systems. *Environmental Science and Pollution Research*, *26*, 31887–31899.

https://doi.org/10.1007/s11356-019-06321-5

Park, J.-H., Ok, Y. S., Kim, S.-H., Cho, J.-S., Heo, J.-S., Delaune, R. D., & Seo, D.-C. (2016). Competitive adsorption of heavy metals onto sesame straw biochar in aqueous solutions. *Chemosphere*, *142*, 77–83.

https://doi.org/10.1016/j.chemosphere.2015.05.093

Patel, P. K., Pandey, L. M., & Uppaluri, R. V. S. (2023). Adsorptive removal of Zn, Fe, and Pb from Zn dominant simulated industrial wastewater solution using polyvinyl alcohol grafted chitosan variant resins. *Chemical Engineering Journal*, *459*, Article 141563.

https://doi.org/10.1016/j.cej.2023.141563

Pepler, P. T. (2009). Assessing arsenic removal by zero valent iron under various water quality and precoat filtration conditions. Master's thesis. University of New Hampshire. https://scholars.unh.edu/thesis/511

Perelomov, L. V, Pinskiy, D. L., & Violante, A. (2011). Effect of organic acids on the adsorption of copper, lead, and zinc by goethite. *Eurasian Soil Science*, *44*, 22–28.

https://doi.org/10.1134/S1064229311010091

Pérez-Marín, A. B., Ortuño, J. F., Aguilar, M. I., Lloréns, M., & Meseguer, V. F. (2024). Competitive effect of zinc and cadmium on the biosorption of chromium by orange waste. *Processes*, *12*(148).

https://doi.org/10.3390/pr12010148

Pérez-Novo, C., Pateiro-Moure, M., Osorio, F., Nóvoa-Muñoz, J. C., López-Periago, E., & Arias-Estévez, M. (2008). Influence of organic matter removal on competitive and noncompetitive adsorption of copper and zinc in acid soils. *Journal of Colloid and Interface Science*, *322*(1), 33–40.

https://doi.org/10.1016/j.jcis.2008.03.002

Pipíška, M., Florková, E., Nemeček, P., Remenárová, L., & Horník, M. (2019). Evaluation of Co and Zn competitive sorption by zeolitic material synthesized from fly ash using 60Co and 65Zn as radioindicators. *Journal of Radioanalytical and Nuclear Chemistry*, *319*, 855–867.

https://doi.org/10.1007/s10967-018-6390-3

Ponthieu, M., Juillot, F., Hiemstra, T., van Riemsdijk, W. H., &

Benedetti, M. F. (2006). Metal ion binding to iron oxides. *Geochimica et Cosmochimica Acta*, *70*(11), 2679–2698.

https://doi.org/10.1016/j.gca.2006.02.021

Rahmani, A. R., Ghaffari, H. R., & Samadi, M. T. (2011). A comparative study on arsenic (III) removal from aqueous solution using nano and micro sized zerovalent iron. *Iranian Journal of Environmental Health Science & Engineering (IJEHSE)*, *8*(2), 175–180. https://www.bioline.org.br/pdf?se11021

Refaey, Y., Jansen, B., Parsons, J. R., De Voogt, P., Bagnis, S., Markus, A., El-Shater, A.-H., El-Haddad, A.-A., & Kalbitz, K. (2017). Effects of clay minerals, hydroxides, and timing of dissolved organic matter addition on the competitive sorption of copper, nickel, and zinc: A column experiment. *Journal of Environmental Management*, *187*, 273–285.

https://doi.org/10.1016/j.jenvman.2016.11.056

Rout, K., Mohapatra, M., & Anand, S. (2012). 2-Line ferrihydrite: synthesis, characterization and its adsorption behaviour for removal of Pb(ii), Cd(ii), Cu(ii) and Zn(ii) from aqueous solutions†. *Dalton Transactions*, *41*(11), 3302–3312.

https://doi.org/10.1039/C2DT11651K

Sağ, Y., Açikel, Ü., Aksu, Z., & Kutsal, T. (1998). A comparative study for the simultaneous biosorption of Cr(VI) and Fe(III) on C. vulgaris and R. arrhizus: application of the competitive adsorption models. *Process Biochemistry*, *33*(3), 273–281.

https://doi.org/10.1016/S0032-9592(97)00060-5

Sağ, Y., & Kutsal, T. (1996). Fully competitive biosorption of chromium(VI) and iron(III) ions from binary metal mixtures by R. arrhizus: Use of the competitive Langmuir model. *Process Biochemistry*, *31*(6), 573–585.

https://doi.org/10.1016/S0032-9592(96)00003-9

Saha, D., Barakat, S., Van Bramer, S. E., Nelson, K. A., Hensley, D. K., & Chen, J. (2016). Noncompetitive and competitive adsorption of heavy metals in sulfur-functionalized ordered mesoporous carbon. *ACS Applied Materials & Interfaces*, *8*(49), 34132–34142.

https://doi.org/10.1021/acsami.6b12190

Santos, A. C. Q., Accioly, A. M. de A., do Nascimento, C. W. A., dos Santos, N. M., Chaves, de M. É. E., & de Lima Xavier, B. T. (2014). Competitive absorption of cadmium, zinc, and lead by velvet bean (Stizolobium aterrimum) and metal distribution among soil fractions. *Communications in Soil Science and Plant Analysis*, *45*(11), 1499–1510.

https://doi.org/10.1080/00103624.2014.904333

Sdiri, A. T., Higashi, T., & Jamoussi, F. (2014). Adsorption of copper and zinc onto natural clay in single and binary systems. *International Journal of Environmental Science and Technology*, *11*, 1081–1092.

https://doi.org/10.1007/s13762-013-0305-1

SenthilKumar, P., Ramalingam, S., Sathyaselvabala, V., Kirupha, S. D., & Sivanesan, S. (2011). Removal of copper(II) ions from aqueous solution by adsorption using cashew nut shell. *Desalination*, *266*(1–3), 63–71.

https://doi.org/10.1016/j.desal.2010.08.003

Seo, J.-H. P., Kim, S.-H., Kang, S.-W., Kang, B.-H., Cho, J.-S., Heo, J.-S., Delaune, R. D., Ok, Y. S., & Seo, D.-C. (2016). Adsorption of Cd, Cu and Zn from aqueous solutions onto ferronickel slag under different potentially toxic metal combination. *Water Science & Technology*, *73*(5), 993–999.

https://doi.org/10.2166/wst.2015.573

Sepehr, E., Piri, M., Ahmadi, F., Gasemi, M., & Sharifmand, M. (2022). Non-competitive and competitive adsorption of cadmium and zinc by nano-iron and titanium oxides from aqueous solution. *International Journal of Environmental Science and Technology*, *19*, 6375–6388.

https://doi.org/10.1007/s13762-021-03833-x

Sepehri, S., Kanani, E., Abdoli, S., Rajput, V. D., Minkina, T., & Lajayer, B. A. (2023). Pb(II) removal from aqueous solutions by adsorption on stabilized zero-valent iron nanoparticles—A green approach. *Water*, *15*(2), Article 222.

https://doi.org/10.3390/w15020222

Shan, R., Shi, Y., Gu, J., Wang, Y., & Yuan, H. (2020). Single and competitive adsorption affinity of heavy metals toward peanut shell-derived biochar and its mechanisms in aqueous systems. *Chinese Journal of Chemical Engineering*, *28*(5), 1375–1383.

https://doi.org/10.1016/j.cjche.2020.02.012

Sheikhhosseini, A., Shirvani, M., & Shariatmadari, H. (2013). Competitive sorption of nickel, cadmium, zinc and copper on palygorskite and sepiolite silicate clay minerals. *Geoderma*, *192*, 249–253.

https://doi.org/10.1016/j.geoderma.2012.07.013

Shuman, L. M. (1977). Adsorption of Zn by Fe and Al Hydrous Oxides as Influenced by Aging and pH. *Soil Science Society of America Journal*, *41*(4), 703–706.

https://doi.org/10.2136/sssaj1977.03615995004100040016x

Sipos, P. (2009). Single element and competitive sorption of copper, zinc and lead onto a Luvisol profile. *Central European Journal of Geosciences*, *1*, 404–415.

https://doi.org/10.2478/v10085-009-0035-2

Srivastava, P., Singh, B., & Angove, M. (2005). Competitive adsorption behavior of heavy metals on kaolinite. *Journal of Colloid and Interface Science*, *290*(1), 28–38.

https://doi.org/10.1016/j.jcis.2005.04.036

Stietiya, M. H., & Wang, J. J. (2014). Zinc and cadmium adsorption to aluminum oxide nanoparticles affected by naturally occurring ligands. *Journal of Environmental Quality*, *43*(2), 498–506.

https://doi.org/10.2134/jeq2013.07.0263

Tarekegn, M. M., Hiruy, A. M., & Dekebo, A. H. (2021). Nano zero valent iron (nZVI) particles for the removal of heavy metals (Cd2+, Cu2+ and Pb2+) from aqueous solutions. *RSC Advances*, *11*(30), 18539–18551.

https://doi.org/10.1039/d1ra01427g

Tessier, A., Rapin, F., & Carignan, R. (1985). Trace metals in oxic lake sediments: possible adsorption onto iron oxyhydroxides. *Geochimica et Cosmochimica Acta*, *49*(1), 183–194.

https://doi.org/10.1016/0016-7037(85)90203-0

Trivedi, P., & Axe, L. (2001). Ni and Zn sorption to amorphous versus crystalline iron oxides: Macroscopic studies. *Journal of Colloid and Interface Science*, *244*(2), 221–229.

https://doi.org/10.1006/jcis.2001.7970

Ugwu, E. I., & Agunwamba, J. C. (2022). Competitive adsorption of copper, zinc, and chromium from wastewater using corn-cob ash: Optimization approach. *International Journal of Engineering Research in Africa*, *58*, 77–94.

https://doi.org/10.4028/www.scientific.net/JERA.58.77

Wang, F., Pan, Y., Cai, P., Guo, T., & Xiao, H. (2017). Single and binary adsorption of heavy metal ions from aqueous solutions using sugarcane cellulose-based adsorbent. *Bioresource Technology*, *241*, 482–490.

https://doi.org/10.1016/j.biortech.2017.05.162

Wang, H. Y., & Huang, H. F. (2010). Competitive adsorption of lead, copper and zinc ions on polymeric Al/Fe modified clinoptilolite. *Advanced Materials Research*, *156–157*, 900–907.

https://doi.org/10.4028/www.scientific.net/AMR.156-157.900

Wang, Y.-Y., Liu, Y.-X., Lu, H.-H., Yang, R.-Q., & Yang, S.-M. (2018). Competitive adsorption of Pb(II), Cu(II), and Zn(II) ions onto hydroxyapatite-biochar nanocomposite in aqueous solutions. *Journal of Solid State Chemistry*, *261*, 53–61.

https://doi.org/10.1016/j.jssc.2018.02.010

Wang, Z., Li, W., Wang, L., Zhang, Y., Li, J., & Liu, Y. (2023). Adsorption of Zn(II), Pb(II), and Cu(II) by residual soil-derived zeolite in single-component and competitive systems. *Sustainability*, *15*(18), 13515.

https://doi.org/10.3390/su151813515

Wang, Z., Wu, X., Luo, S., Wang, Y., Tong, Z., & Deng, Q. (2020). Shell biomass material supported nano-zero valent iron to remove Pb2+ and Cd2+ in water. *Royal Society Open Science*, *7*(10), Article 201192.

https://doi.org/10.1098/rsos.201192

Wei, Q., He, R., Sun, H., Ding, Y., Wang, C., Ma, X., & Yang, G. (2024). Competitive adsorption of copper and zinc ions by Tetradesmus obliquus under autotrophic and mixotrophic cultivation. *Journal of Water Process Engineering*, *60*, Article 105201.

https://doi.org/10.1016/j.jwpe.2024.105201

Wu, F., Zhao, C., Qu, G., Yan, Z., Zeng, Y., Chen, B., Hu, Y., Ji, W., Li, Y., & Tang, H. (2021). Adsorption of arsenic from aqueous solution using a zero-valent iron material modified by the ionic liquid [Hmim]SbF6. *RSC Advances*, *11*(12), 6577–6585.

https://doi.org/10.1039/D0RA09339D

Xue, C., Zhu, L., Lei, S., Liu, M., Hong, C., Che, L., Wang, J., & Qiu, Y. (2020). Lead competition alters the zinc adsorption mechanism on animal-derived biochar. *Science of The Total Environment*, *713*, Article 136395.

https://doi.org/10.1016/j.scitotenv.2019.136395

Xue, Y., Hou, H., & Zhu, S. (2009). Competitive adsorption of copper(II), cadmium(II), lead(II) and zinc(II) onto basic oxygen furnace slag. *Journal of Hazardous Materials*, *162*(1), 391–401.

https://doi.org/10.1016/j.jhazmat.2008.05.072

Xue, Y., Hu, Z., & Niu, Y. (2020). Single and coadsorption of copper, cadmium, lead and zinc onto basic oxygen furnace slag. *Desalination and Water Treatment*, *179*, 242–251.

https://doi.org/10.5004/dwt.2020.24868

Yan, M., Fang, W., Feng, H., Zhang, Y., Wibowo, H., Kanchanatip, E., & Ar Rahim, D. (2024). Performance evaluation of Zn-Fe adsorbent for H2S adsorption during biogas purification. *Biomass Conversion and Biorefinery*, *14*, 8321–8331.

https://doi.org/10.1007/s13399-022-02959-3

Yang, M., Lu, C., Zhang, S., Wang, Y., Xu, R., Zhang, M., Wen, J., & Li, Z. (2024). Concurrent removal of Fe(II), Cu(II), and Zn(II) cations from acid mine drainage by an industrial solid waste - Steel slag: Behaviors and mechanisms. *Environmental Research*, *263*(Part 2), Article 120105.

https://doi.org/10.1016/j.envres.2024.120105

Youssef, N. A., Shaban, S. A., Ibrahim, F. A., & Mahmoud, A. M. (2017). Preparation of nano-Fe2O3 particles and evaluation of their catalytic activity in adsorption of Pb(II), Mn(II) and Zn(II) from aqueous solution. *Desalination and Water Treatment*, *69*, 284–293.

https://doi.org/10.5004/dwt.2017.0477

Zhang, G., Yang, H., Zhao, T., Li, X., Zhou, Y., & Guo, S. (2022). Highly efficient removal of As(III), Zn(II), Cu(II) and Cd(II) in aqueous solution using thermal desorption residue from oil sludge contaminated soil: Performance and mechanism. *Journal of Environmental Chemical Engineering*, *10*(3), Article 107668.

https://doi.org/10.1016/j.jece.2022.107668

Zhang, M., Wang, H., McDonald, L. M., & Hu, Z. (2017).

Competitive biosorption of Pb(II), Cu(II), Cd(II) and Zn(II) using composted livestock waste In batch and column experiments. *Environmental Engineering & Management Journal (EEMJ)*, *16*(2), 431–438.

https://doi.org/10.30638/eemj.2017.043

Zhao, D., Wang, Z., Lu, S., & Shi, X. (2020). An amidoxime-functionalized polypropylene fiber: Competitive removal of Cu(II), Pb(II) and Zn(II) from wastewater and subsequent sequestration in cement mortar. *Journal of Cleaner Production*, *274*, Article 123049.

https://doi.org/10.1016/j.jclepro.2020.123049

Zhu, H., Shi, M., Zhang, X., Liu, B., & Yao, D. (2020). Adsorption kinetics of arsenic (V) on nanoscale zero-valent iron supported by activated carbon. *Nanomaterials*, *10*(9), Article 1791.

https://doi.org/10.3390/nano10091791